THE UNION REEFS PROSPECT, N.T.: STRUCTURE AND GEOCHEMISTRY OF A TURBIDITE HOSTED GOLD DEPOSIT.

by
John S. Donaldson B.Sc.

A research thesis submitted
in partial fulfilment of the degree
Bachelor of Science with Honours.

Centre for Ore Deposit and Exploration Studies,
University of Tasmania,
December, 1992

"There's a lady who's sure all that glitters is gold..."

(Robert Plant, Led Zeppelin)

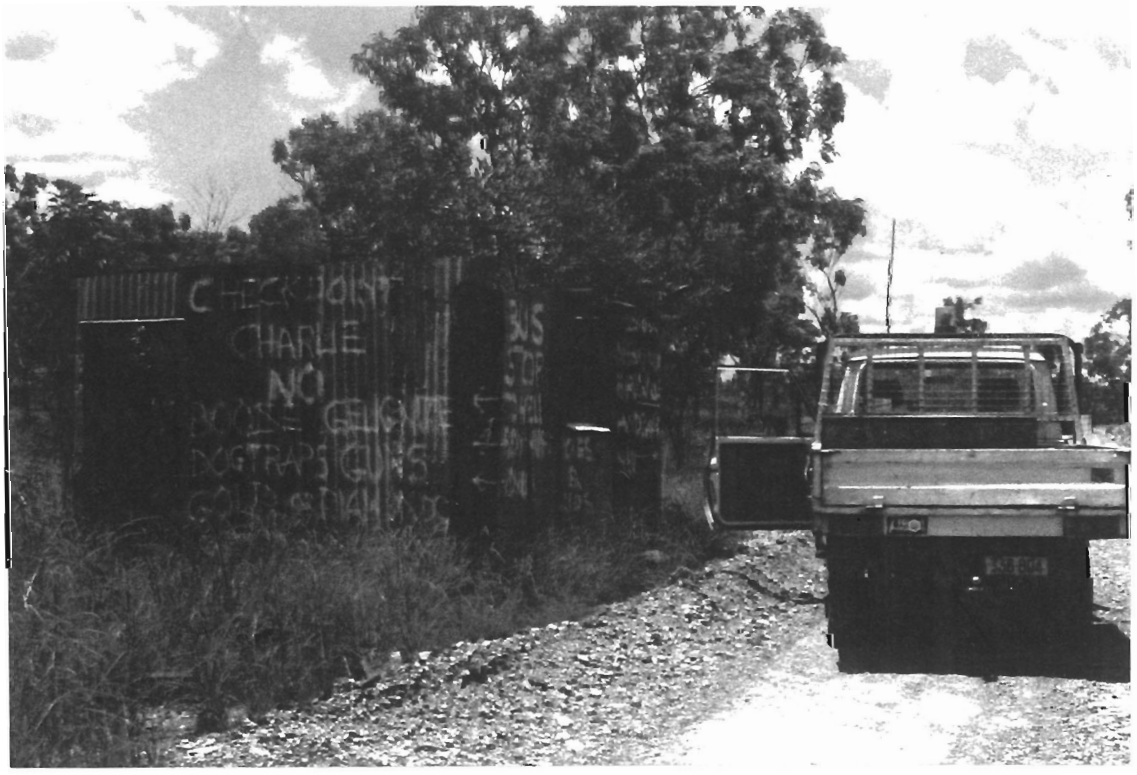

ABSTRACT

The Union Reefs gold prospect is located approximately 15.5 km north-west of Pine Creek, in the Northern Territory. It is hosted within the Burrell Creek Formation, a Palaeoproterozoic turbidite sequence of the Pine Creek Geosyncline.

Two deformations have been recognised at the prospect. The first deformation produced tight folds and a continuous slaty cleavage. The second deformation produced long wavelength folds, mesoscopic folds, a discontinuous spaced and crenulation cleavage, and conjugate kinks. A domal structure was produced from fold interference.

The mineralisation event occurred during the second deformation. It is associated with breccia zones and quartz sulphide veins, and crosscuts buck quartz veins and sheeted quartz veins. Mineralisation consists of pyrrhotite, arsenopyrite, marcasite, pyrite, chalcopyrite, sphalerite, galena, gold, bismuth, bismuthinite and an unidentified phase.

Based on data derived from field observations, petrographic studies and sulphur isotope analyses, a genetic model for gold mineralisation at the prospect is proposed. The genetic model suggests that sulphur was derived from a mixed igneous and sedimentary source. Gold was sourced from the sedimentary pile by fluids convecting under elevated temperature in response to emplacement of the Allamber Springs Granite. The convecting fluids were focussed into dilatant structures within uplifted, fault bounded blocks and corridors. Deposition of gold is thought to be a result of a decrease in the oxygen fugacity of the gold bearing fluid.

ACKNOWLEDGMENTS

The author wishes to thank Billiton Australia Pty. Ltd. for providing logistical support and making the project possible. I extend my sincerest thanks to Dave Wegmann of Billiton Australia Pty. Ltd. and Kim Hein for proposing the topic.

I am most grateful to Dr. Richard Keele for his supervision, advice and useful criticism throughout the year.

I am very grateful to Renison Goldfields Consolidated for the scholarship which provided a financial basis for the year.

I would also like to thank the staff at Billiton Australia Pty. Ltd. Darwin office, particularly Dave Wegmann, Craig Mackay, Ken Hellsten, Elaine Wakefield, Ruth, Harry, Barb and Brad.

I am deeply indebted to the staff and students of CODES and the Geology Department. In particular I would like to thank Dr. Dave Huston and Dr. Khin Zaw for their advice and help.

Thanks to Jamie Rogers for undertaking a totally useless (well almost) magnetic susceptibility profile, and for all his help generally. Best I don't forget my honours comrades - Stumpy, Abster, Jimbo, Matt, Russel, Mark and John - not only for the borrowing of various items, but for being good mates. Also I would like to thank Pete Kaliniecki for useful discussions on rocks and life.

I am grateful to Deborah Harding for drafting my maps, and for not freaking out too much when the map required redrafting.

Thanks to my family for their support throughout the year, especially my father for his regular pre-exam advice.

If I were to thank Kim Hein for all her effort and input it would require the writing of a separate thesis. I don't know how you put up with me, but I am glad you did. Now it's my turn.

CONTENTS

CHAPTER 4 - STRUCTURE AND METAMORPHISM

CHAPTER 5 - MINERALISATION

CHAPTER 6 - SULPHUR ISOTOPES

CHAPTER 7 - GEOCHEMICAL MODEL FOR MINERALISATION

LIST OF FIGURES

CHAPTER 5

CHAPTER 6

LIST OF TABLES

CHAPTER 1

INTRODUCTION

1.1 Location and physiography

The Union Reefs gold prospect, latitude 13° 42' S, longitude 131°47' E, is situated approximately 185 km southeast of Darwin and 13.5 km north-northwest of Pine Creek in the Cullen Mineral Field, Northern Territory, Australia (AMG co-ordinates: 8482500 m N, 780130 m E) (Figure 1.1). It is wholly incorporated within the 1:250 000 scale Cullen Mineral Field sheet (Stuart-Smith, 1987) and the 1:100 000 Pine Creek sheet (Stuart-Smith *et al.*, 1987).

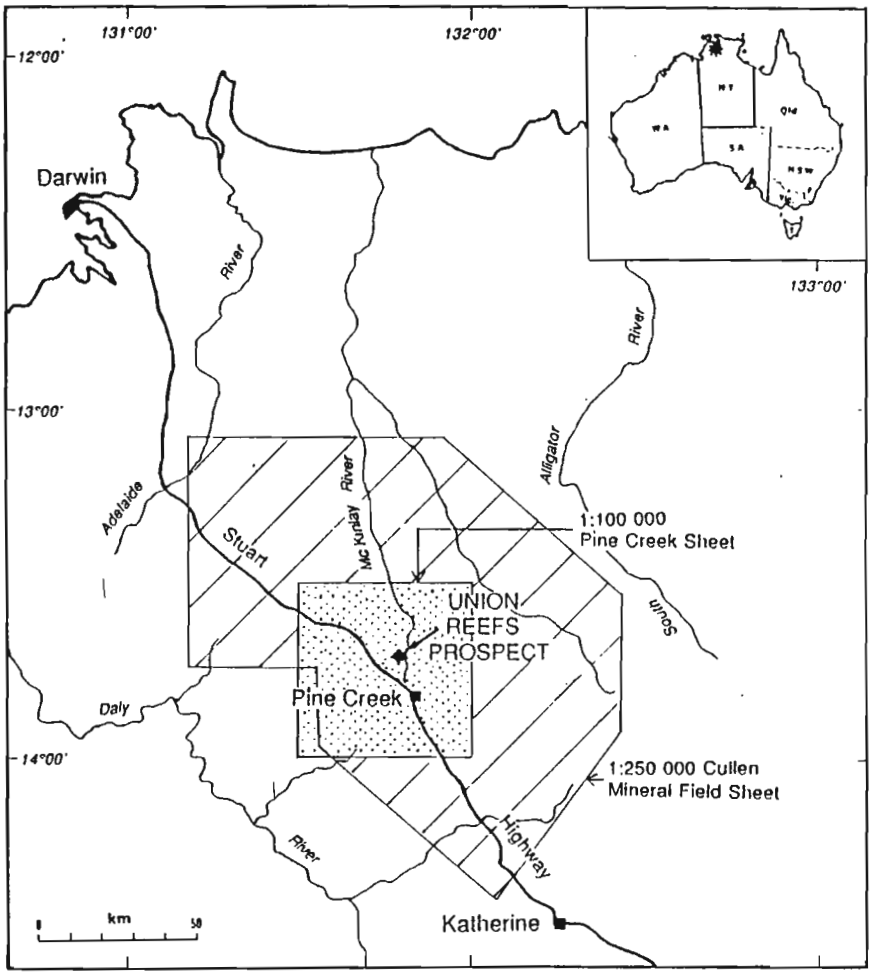

FIGURE 1.1: Location of the Union Reefs gold prospect.

The area is generally accessible from the Stuart Highway by a gravel road which may be inaccessible during the months of November-February due to flooding at the McKinlay River crossing.

Vegetation in the area may be termed tropical savanna woodland, and consists of various Eucalypt species with spear grass (sorghum) dominant in the understorey.

Historical workings occur on two sub-parallel rocky ridges which run approximately north-northwest for over 4 km. The resistant nature of the ridges results from numerous quartz veins within them. To the east of the prospect a 250 m high ridge of hornfelsed rock overlooks the area. Low lying areas are blanketed by alluvium, while colluvium is found on the slopes and crests of hills.

1.2 Mining and exploration history

The Union Reefs prospect was discovered in December 1873 (Turner, 1990), and since that time approximately 1600 pits, shafts, adits and open cuts have been worked (Shields *et al.*, 1967). Gold mining began prior to 1884, although no records have been found to quantify the amount of gold extracted.

Hossfeld (1936) stated that up until 1892, the leases over the Union Reefs prospect were held by European and Chinese miners. The companies working at the prospect at that time were the South Union Gold Mining Company, the Alice Hills Gold Mining Company, and the Union Gold Mining Company. After 1892 the leases had been purchased or tributed by Chinese miners, 120 of whom were working at Union Reefs in 1894. Incomplete records show that for the period 1884 to 1910, 58,232 tons of crushed ore yielded 1363.8 kg of gold, and 3,900 tons of cyanide treated ore yielded 13.4 kg of gold. By 1910 significant production had ceased, possibly because remaining payable ore had been worked to water level and/or picked from old mullock heaps. However, six government funded diamond drill holes were sunk between 1905 and 1914 (Jensen, 1915; Hossfeld, 1936; Shields *et al.*, 1967).

The Union Reefs prospect was re-examined by the Bureau of Mineral Resources from 1963 to 1964. The area was mapped and 13 diamond holes were drilled. TEM and IP geophysical surveys were conducted and a resource at Crosscourse was identified (Shields *et al.*, 1967). In 1969 and 1970 Central Pacific Minerals N.L. drilled four diamond holes (Shields, 1970), and in 1984 and 1988, 25 exploration

and delineation holes were drilled by Enterprise Gold Mines N.L. (Baxter, 1987; Turner, 1990). Despite knowledge of the Crosscourse resource, activity at the prospect was minimal.

In 1991 the leases at Union Reefs were acquired by Billiton Australia Pty. Ltd. who have undertaken diamond and face return percussion drilling, soil sampling, geophysical surveys and metallurgical test work in order to assess the feasibility of open cut mining at Crosscourse.

Leases over alluvial operations in the west of the Union Reefs prospect are currently held by Togar Pty. Ltd..

1.3 Aims

The main aims of this study were:-

(1) To map and describe the geology of the Union Reefs prospect.
(2) To erect a local stratigraphic sequence for the immediate vicinity of the prospect.
(3) To map and describe the structures in the prospect and to propose a structural history, with specific reference to vein formation.
(4) To propose a paragenetic sequence in relation to gold mineralisation.
(5) To examine the geochemistry of mineralising fluids and deduce a possible source for the fluids.
(6) To examine the structural and lithological controls on gold mineralisation.
(7) To propose a genetic model for gold mineralisation.

1.4 Methods

Geological mapping at 1:5000 scale over the Union Reefs prospect involved traverses along and across the strike, following individual contacts and structures, as well as taking spot readings. A detailed geological fact map at 1:5000 scale (Figure 1.2) was produced from this work. Interpretation of this map in conjunction with a 1:5000 scale aerial photo allowed the development of a lithological and structural interpretation map at 1:5000 scale, with a stratigraphic column (Figure 1.3), and three cross-sections at 1:5000 scale (Figure 4.14). Regional investigations focussed on granite-sediment contacts.

Forty-one field samples were collected from the Union Reefs prospect and from its immediate vicinity. A further 46 samples were collected from diamond drill core. Twenty-five polished thin sections, 13 thin sections and 4 polished blocks were made from these samples and examined petrographically in order to classify igneous and sedimentary lithologies, and to establish a paragenetic sequence for gold mineralisation.

Structural data was analysed using equal area stereoprojections and rose diagrams. Further structural observations were made from orientated field samples, thin sections and photographs taken in the field.

Sulphur isotope $\delta^{34}S/\delta^{32}S$ ratios were measured on SO_2 gas obtained from 14 pyrite, 7 arsenopyrite, 5 pyrrhotite, 3 sphalerite and one chalcopyrite sample (30 in total), using the method of Robinson and Kusakabe (1975). Sulphide samples were collected from DDH UJ9, UK15, URD007, URD008 and URD009 from the Crosscourse and Ping Ques' areas.

1.5 Terminology and Notation

The terms "Palaeoproterozoic", "Mesoproterozoic" and "Neoproterozoic" are used in accordance with IUGS-approved chronometric subdivision for the Precambrian time and Proterozoic Eon, as proposed by Plumb (1991).

The term "Union Reefs prospect" refers to the area covered by Figures 1.2 and 1.3. The term "Pine Creek area" refers to that area in Figure 2.3 . "Union North", "Union Central", "Union South", "Crosscourse", "Ping Ques'", "Lady Alice North", "Lady Alice", "Lady Alice South", "Millars'" and the "Dam" all refer to regions within the Union Reefs prospect. "Union line" and "Lady Alice line" refer to the entire western and eastern line of historical workings, respectively, in the Union Reefs prospect.

Sedimentary and igneous rocks are classified according to Ehlers and Blatt (1982). "Siltstone/shale" is used to denote siltstone interbedded with shale and together with the terms "sandstone greywacke" and "gritstone marker" are field terms for units whose characteristics are described in Chapter 3.

V_a, V_b, V_c, and V_d are field terms for quartz veins whose characteristics are described in Chapter 5 and have no genetic or structural implication. The term "Broken China Anticline" refers to that anticlinal structure indicated in Figure 1.3.

Foliations are classified according to Gray (1977) and Powell (1979). The symbols used to denote foliations and folds are S_n and F_n respectively, with the symbol D_n used to denote the deformation interpreted as being responsible for their development. The relative age of each deformation is denoted by the subscript n, the earliest phase recognised being D_1. S_0 is used to denote bedding. Field measurements are plotted to magnetic north, which is 16° anticlockwise of true north and 21° anticlockwise of grid north.

TABLE 1.1: NOTATION

SYMBOL	MEANING
µm	micrometres
mm	millimetres
cm	centimetres
m	metres
km	kilometres
kb	kilobars
°C	degrees Celsius
Ma	million years ago
DDH	diamond drill hole
TM	turam indicator
TEM	time domain electromagnetism
IP	induced polarisation

CHAPTER 2

REGIONAL SETTING

2.1 Regional geology

The Union Reefs prospect is located in the southern central region of the Central Domain (Figure 2.1) of the Pine Creek Inlier, and is hosted in Palaeoproterozoic sediments of the Burrell Creek Formation. The Pine Creek Inlier consists of a sequence of geosynclinal sediments and volcanics which were deformed, metamorphosed and intruded by syn- to post-orogenic granitoids (eg., the Cullen Batholith) during the Top End Orogeny. The deformed rocks of the Inlier are unconformably overlain by relatively undeformed Palaeoproterozoic, Mesoproterozoic, Neoproterozoic and Phanerozoic sediments (Figure 2.1).

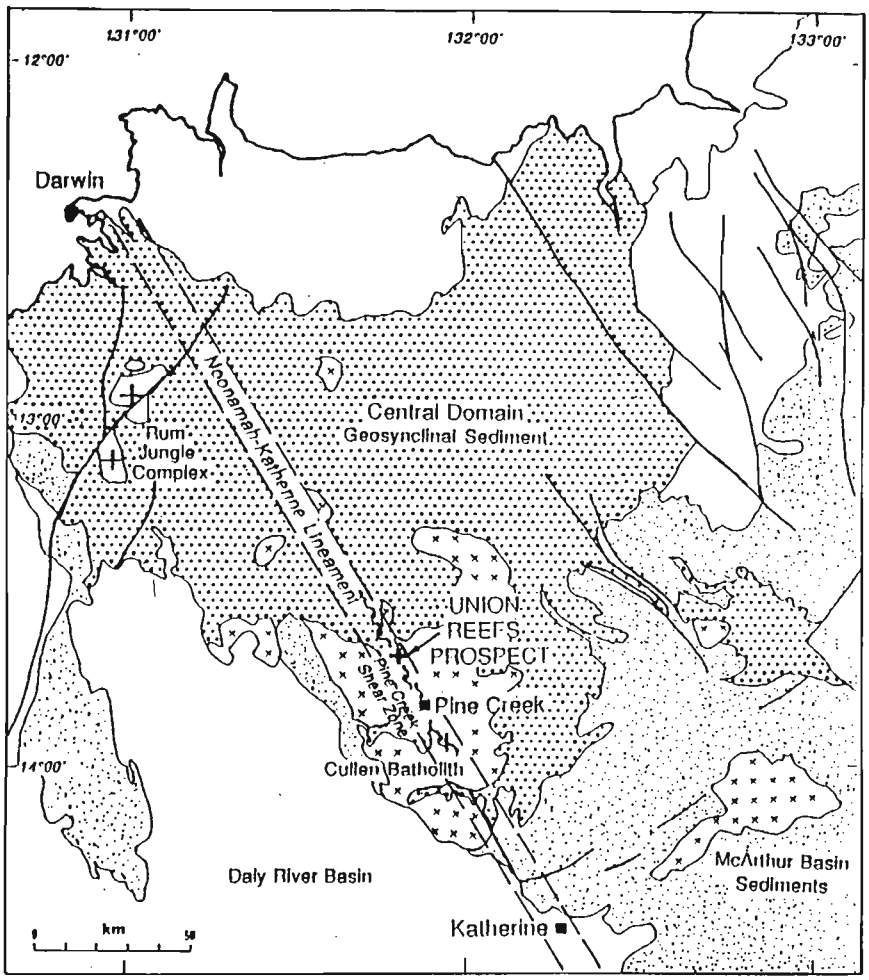

FIGURE 2.1: Generalised geology of the Pine Creek Inlier. Modified after Needham and Stuart-Smith (1985a, Figure 1, pp. 233).

Basement rocks of the Pine Creek Inlier are unconformably overlain by sediments of the Pine Creek Geosyncline and consist of gneisses and granitic rocks, with minor metasedimentary units (Needham *et al.*, 1988). They outcrop in the western region of the Central Domain, approximately 50 km south of Darwin (Figure 2.1). Richards *et al.* (1977) determined an age older than 2400 Ma (Rb-Sr whole rock age) for parts of the Rum Jungle complex.

The Pine Creek Geosyncline consists of pelitic sediments (approximately 75%) which are commonly carbonaceous, with lesser psammites and carbonates (approximately 10%), rudites (approximately 5%) and volcanics (approximately 10%) (Needham *et al.*, 1980). The sediments represent a sequence deposited approximately 1900 Ma ago in an intra-cratonic basin under alternating continental and shallow marine environments (Needham *et al.*, 1988).

Needham *et al.* (1988) divided the sediments into three discrete phases (Figure 2.2); a rift phase, a sag phase, and a pre-orogenic phase. The rift phase sediments include the Namoona and Mount Partridge Groups, which are quartz rich sediments that contain minor bimodal volcanics. The sediments represent fluviatile activity developed during the initial stage of crustal extension. The sag phase sediments, represented by the South Alligator Group, consist of distal pelitic sediments and proximal carbonates. They relate to sagging associated with post-extension subsidence and unconformably overlay the rift phase sediments. The pre-orogenic phase is represented by sediments of the Finniss River Group (Burrell Creek Formation) and conformably overlie the sag phase sediments. These sediments represent uplift of distal provenances and herald the onset of the Top End Orogeny.

Between 1870 and 1690 Ma the Pine Creek Inlier underwent a period of compressional and extensional tectonism known as the Top End Orogeny. The Orogeny consisted of three compressional events; the Nimbuwah Event, the Maud Creek Event and the Shoobridge Event. The principal phase of compression took place during the Nimbuwah Event which has been dated by Page and Williams (1988) at 1885 to 1870 Ma. The Nimbuwah Event correlates with the Barramundi Orogeny of northern Australia as described by Etheridge *et al.* (1987). Compressional tectonism was accompanied by low grade regional metamorphism and uplift and erosion.

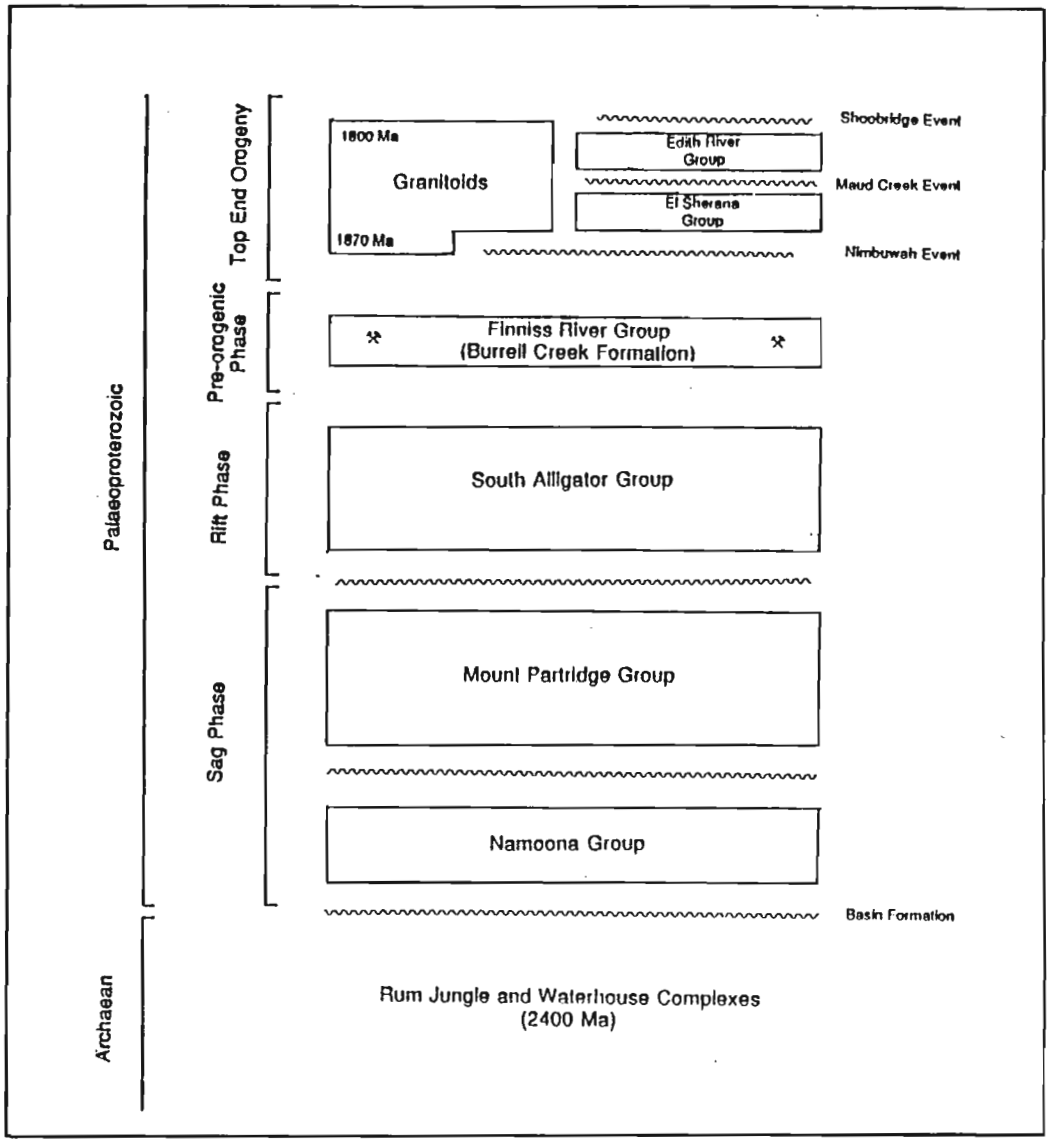

FIGURE 2.2: Simplified stratigraphy of the Central Domain of the Pine Creek Inlier, plus tectonic Events. Modified after Needham *et al.* (1988, Figure. 5, pp. 348).

Extensional tectonism was accompanied by the deposition of volcanoclastic and flyschoid sediments of the El Sherana Group into shallow north-westerly trending grabens, which were subsequently folded and faulted during the Maud Creek Event (Needham *et al.*, 1988). The felsic volcanics of the Edith River Group were deposited in several basinal structures after graben subsidence was reactivated at the culminating stages of this Event (Needham & Stuart-Smith, 1985b). The

Shoobridge Event was the last regional metamorphic and deformational event of the Top End Orogeny and was characterised by the development, or reactivation of, north-south to north-west to south-east striking shear zones (Needham *et al.*, 1988).

The sediments of the Pine Creek Geosyncline were intruded by syn- to post-orogenic I-type granitoids of the Cullen Batholith between 1870 and 1800 Ma (Needham *et al.*, 1988). The Batholith is the largest granitoid complex in the Pine Creek Inlier and forms a V-shaped body centred around the township of Pine Creek. Stuart-Smith *et al.* (1987) defined fourteen discrete plutons within the Batholith which include monzonites, granodiorites, granites and leucogranites.

The region has been stable since the Neoproterozoic, with minor sedimentation and movement on NW-SE trending structures (Needham *et al.*, 1988).

2.2 Regional structures

Deformation and metamorphism of the Pine Creek Geosyncline during the Top End Orogeny produced tight to isoclinal folding and extensive faulting (Stuart-Smith *et al.*, 1987). Johnson (1984) suggested five deformations were associated with this event; bedding parallel foliation (D_1), recumbent mainly west-verging folds (D_2), upright NNW-SSE trending folds (D_3), easterly tight folds (D_4), and a late kink foliation (D_5). D_3 and D_4 correlate with D_1 and D_2 in the Pine Creek area.

F_1 folds are tight to isoclinal, while F_2 folds are widely spaced and of long wavelength (Stuart-Smith *et al.*, 1987). F_1 folds trend north to north-west (Figure 2.3), are symmetrical, and are upright to inclined to the south-west, commonly with overturned limbs (Stuart-Smith *et al.*, 1987). F_2 folds trend east and may be associated with poorly developed mesoscopic kink or crenulation cleavages with an easterly trend (Stuart-Smith *et al.*, 1987). The intrusion of the Cullen Batholith, and development of the Pine Creek Shear Zone modified these structures (Stuart-Smith *et al.*, 1987).

Folding in the Pine Creek area is locally modified by the Pine Creek Shear Zone (Figure 2.3), and by faults up to 20 km long which have displacements in the order of a few metres to 1 km (Stuart-Smith *et al.*, 1987). The Pine Creek Shear Zone is a major northwesterly-trending wrench fault system which was active before and after granitoid emplacement (Stuart-Smith, 1985). The Shear Zone is contained within the north-west trending Noonamah-Katherine Lineament (Simpson et al.,

1980) which has a coincident TM signature, magnetic and gravity anomaly. Stuart-Smith *et al.* (1987) suggested that movement on the Shear was sinistral and in the order of 1 to 2 km, while experimental work by Krowkowski and Olissoff (1990) indicated that movement involved sinistral transpression. They added that a sinistral transpression was followed by a late phase of dextral-strike slip activity.

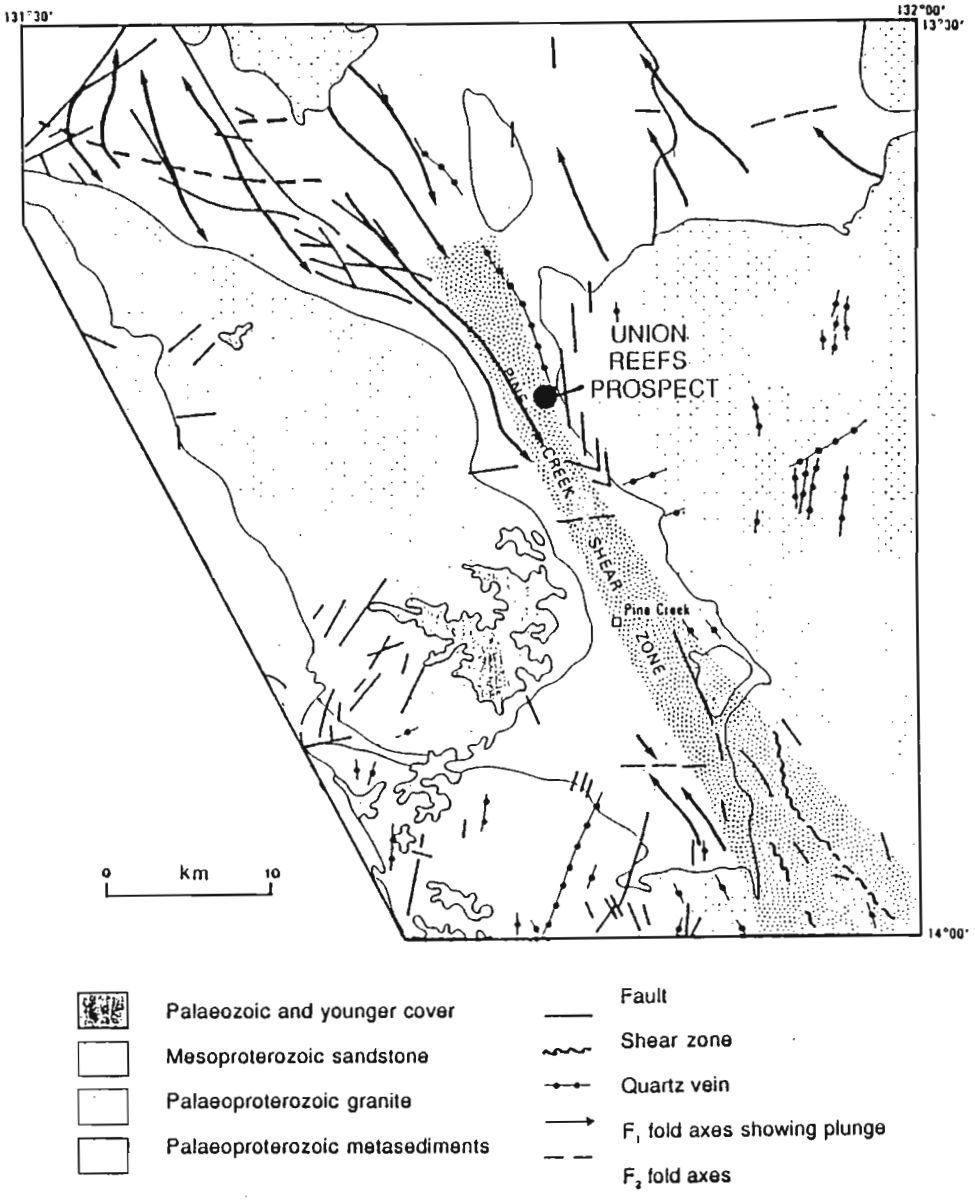

FIGURE 2.3: Folding, faults and shear zones in the Pine Creek area. Modified after Stuart-Smith *et al.* (1987, Figure 6 & 7, pp. 26-27).

2.3 Local setting of the Union Reefs prospect

The Union Reefs prospect is located within a corridor of Palaeoproterozoic metasediments which is flanked to the east and west by lobes of the Cullen Batholith. The north-west trending corridor contains sediments of the Burrell Creek Formation and is approximately 5 km wide at the prospect (Figure 2.4).

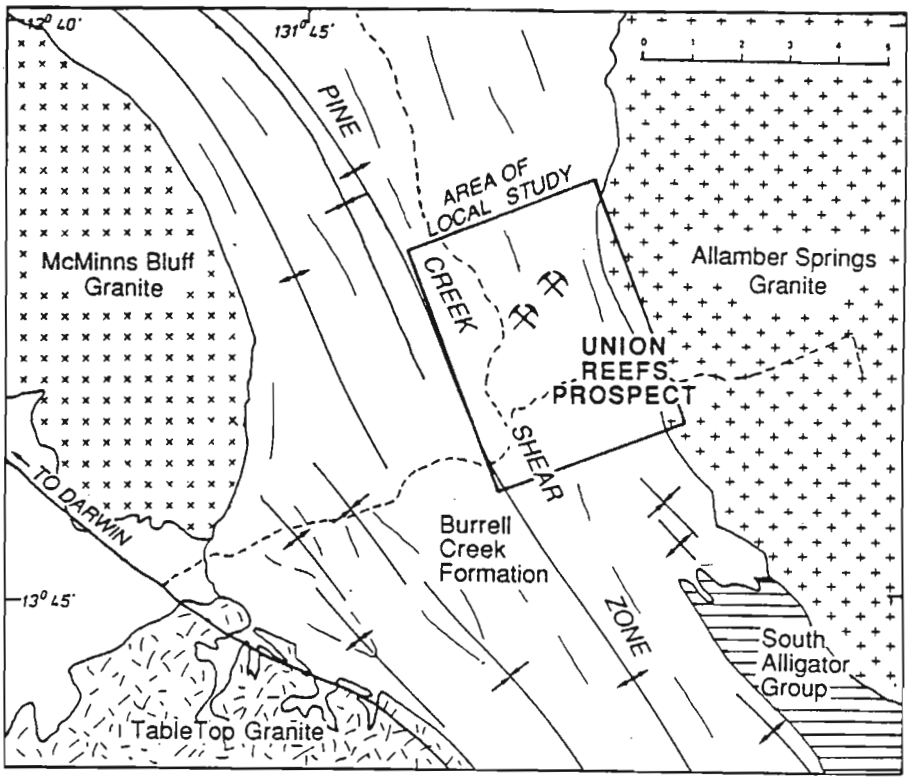

Figure 2.4: The geological setting of the Union Reefs prospect.
(Modified after Stuart-Smith *et al.*, 1987.)

The Burrell Creek Formation consists of turbiditic sediments of siltstone, shale, sandstone, and minor arkose, quartzite, conglomerate and schists. The Formation is the only member of the Finniss River Group and the youngest unit of the Pine Creek Geosyncline.

The Allamber Springs Granite, the McMinns Bluff Granite and the Tabletop Granite, are those plutons of the Cullen Batholith which are most closely associated with the Union Reefs prospect. Stuart-Smith and Page (1991) recorded that the McMinns

Bluff Granite (1835±6 Ma, U-Pb zircon age) was significantly older than the Allamber Springs Granite (1818-1825 Ma, U-Pb zircon age). Furthermore, Stuart-Smith *et al.* (1987) suggested that the McMinns Bluff Granite was older than the Tabletop Granite.

The Pine Creek Shear Zone is approximately 2.5 km wide at the Union Reefs prospect.

CHAPTER 3

LITHOLOGIES

3.1 Burrell Creek Formation

3.1.1 Sandstone greywacke and siltstone/shale

Sandstone greywacke units are characterised in the field by those rocks which contain clasts visible with a hand lens. Bedding is well defined and ranges in thickness from approximately 5 cm, to greater than 30 cm. Less commonly bedding is massive and up to 1 m thick. Siltstone/shale is characterised by those rocks containing clasts which were not visible with a hand lens. Bedding occurs as one of two general types; (i) very thin to thinly bedded, ranging in thickness from approximately 1 to 5 cm, or, (ii) thickly laminated, approximately 0.5 mm thick laminations.

In the oxidised zone the rocks vary in colour from olive green to brown, orange, red and purple. In diamond drill core they range in colour from light grey to greenish-black below the oxidised zone. The darker colours indicate a reducing environment for deposition of these sediments.

Turbiditic sedimentary features, associated with classical turbidites (Walker, 1984), are common throughout the prospect. The features at the mesoscopic and megascopic scale were used extensively in determining sedimentary facing. Sandstone greywacke and siltstone/shale are monotonously interbedded along the entire stratigraphic section of approximately 580 m (Figure 1.3 and Figure 3.1). Beds of sandstone greywacke displayed sharp, irregular contact with underlying units and commonly graded upward into finer grained sandstone greywacke and/or siltstone/shale, which are often well laminated, ie., divisions A and B of the Bouma sequence. Graded bedding, cross-bedding, flames and ripple marks are also commonly observed. A north-westerly palaeocurrent flow direction is indicated by north-easterly striking ripple marks at Lady Alice North.

The sandstone greywacke and siltstone/shale of the prospect generally exhibited fining upwards in stratigraphic sequence. This feature can be observed over stratigraphic intervals of a few metres to 50 m, and indeed over the entire stratigraphic thickness. Lower stratigraphic intervals are dominated by sandstone greywacke with minor siltstone/shale, while higher stratigraphic intervals are dominated by siltstone/shale (Figure 1.3 & Figure 3.1).

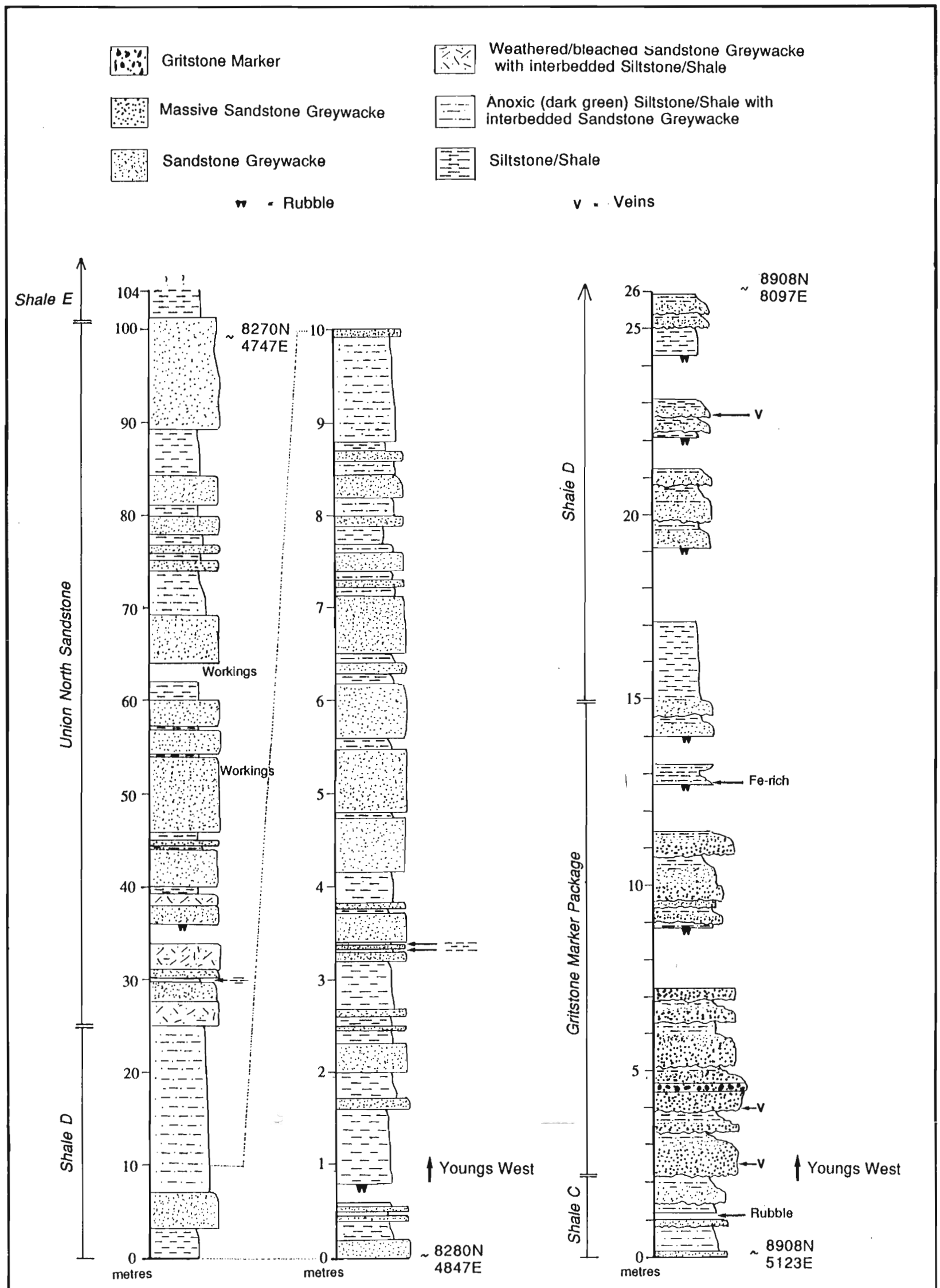

Figure 3.1: Stratigraphic intervals of the Burrell Creek Formation at the Union Reefs prospect.

Petrographically, the sediments are poorly sorted and range from very fine siltstone to sandy coarse siltstone. Sub-angular to angular clasts range in size from approximately 25 μm to 800 μm and consist of quartz, chert, plagioclase, potassium feldspar and composite clasts of quartz and feldspar. The matrix consists of quartz, sericite and chlorite plus minor biotite, magnetite, apatite, tourmaline and titanium relicts, and detrital zircon, biotite, and hornblende. Grain size ranges from approximately 5 μm to 50 μm.

3.1.2 Gritstone marker

A gritstone marker bed crops out intermittently at the Union Reefs prospect, most commonly along the Union line. The bed is a fine pebble conglomerate approximately 5-8 cm in thickness and commonly occurs within a massive sandstone greywacke bed approximately 1 m in thickness. These two beds occur within the centre of a sandstone greywacke unit that varies in thickness from 15-40 m, termed the "Gritstone Marker Package". This unit was used extensively to correlate units throughout the prospect.

The gritstone marker bed contains rounded to sub-angular, matrix supported, quartz and chert clasts to 5 mm in diameter. Quartz clasts are often polycrystalline and/or have undulose extinction. The matrix consists of quartz, sericite and chlorite. Occasional disseminated chalcopyrite anhedra, up to 2 mm, are preserved.

The gritstone marker bed is sheared and a strong foliation is developed parallel to the strike of the bed. Thin quartz veins, approximating 0.05 mm in width, and zones of sericite, approximating 1 to 3 mm in width, are parallel to the foliation. The foliation wraps around larger clasts and smaller clasts appear rotated into parallelism with this foliation.

3.1.3 Stratigraphic sequence

The stratigraphic sequence at the Union Reefs prospect is informally named as follows; the lowest unit is the Lady Alice Sandstone, this is followed in sequence by Shale A, the Central Sandstone, Shale B, the Dam Sandstone, Shale C, the Gritstone Marker Package, Shale D, the Union North Sandstone, Shale E, the Western Sandstone and Shale F. Siltstone/shale units, less than 15 m thick, occur within the Lady Alice Sandstone, the Gritstone Marker Package and the Union North Sandstone at approximately 5000E 7400N, 4800E 7050N and 4800E 7500N, respectively. This stratigraphic sequence and the approximate thickness of units is given in Figure 1.3.

Known mineralisation is hosted almost exclusively within the Lady Alice Sandstone, the Central Sandstone and the Union North Sandstone (this is discussed further in Section 4.6). Knowledge of position in the stratigraphic sequence would be essential in defining where prospective units may occur and/or rating the prospectivity of units.

3.1.4 Provenance

The provenance of the Burrell Creek Formation at Union Reefs is most likely mixed igneous, metamorphic and volcanic. An alkali igneous provenance is indicated by the presence of potassium feldspar, composite clasts of feldspar and quartz, apatite, tourmaline, titanium relicts, zircon and biotite. The presence of chert, potassium feldspar, polycrystalline quartz and quartz with undulose extinction indicate a metamorphic provenance. A volcanic provenance is indicated from the presence of plagioclase.

3.2 Igneous rocks

3.2.1 Bludells Monzonite

A circular body of dark green/pink monzonite (interpreted as the Bludells Monzonite) crops out approximately 200 m west of Union North. It consists mainly of orthoclase and biotite (2 mm in diameter), bundles of tourmaline needles (5 mm long), and calcite veins (2 mm wide). Andesine/oligoclase ($Ab_{30-40}An$) and chlorite are minor constituents, together with accessory magnetite and rutile. Accessory disseminated sulphides include pyrite, arsenopyrite, chalcopyrite and pyrrhotite. Bismuthinite occurs together with an unidentified phase, their presence suggesting the rock may carry gold, since these minerals are associated with gold in the ore zones (see Chapter 5).

The monzonite is sheared. In outcrop slickenslides are observed, while a foliation is evident petrographically. The foliation is defined by chlorite which fills fractures in calcite veins. The deformed nature of the monzonite appears to support conclusions by Stuart-Smith *et al.* (1987) that the Bludells Monzonite is the oldest, most deformed and altered phase of the Cullen Batholith.

3.2.2 McMinns Bluff Granite

The McMinns Bluff Granite is grey/green in colour and is porphyritic. White potassium feldspar phenocrysts, up to 4 cm in diameter, lie in a groundmass (crystal size approximately 4 mm in diameter) of quartz, oligoclase ($Ab_{30}An$), potassium feldspar, biotite and accessory zircon and opaques. Zircons inclusions in biotite are indicated by the presence of uranium haloes. Quartz exhibits undulose extinction.

The granite-sediment contact occurs approximately 5 km west of the Union Reefs prospect. Here the granite is rich in mica and feldspar. The sediment is hornfelsed and heavily weathered to a mottled white/grey and brown/red colour. Brown aplite dykes, approximately 30 cm wide occur within the granite close to its contact with the sediments. Xenoliths, approximately 40 cm in diameter, also occur.

3.2.3 Allamber Springs Granite

The Allamber Springs Granite is pink in colour and is equigranular. It consists of coarse crystals (to 5 mm) of quartz, andesine ($Ab_{35}An$), microcline, potassium feldspar, and biotite plus accessory fluorite, and chlorite. Quartz exhibits undulose extinction and is recrystallised at its crystal margins.

The contact aureole of the Allamber Spring Granite contains 40 cm wide granitic dykes which consist of potassium feldspar, quartz, tourmaline and mica. The dykes do not extend beyond 200 m of the granite-sediment contact.

A brecciated silicified hornfels (1 m wide) crops out parallel to, and within approximately 50 m of the contact. Fragments of silicified hornfels are fawny brown in colour and up to 5 cm in diameter. The fragments display a jigsaw texture and are surrounded by a dark grey silicic matrix suggesting that the rock was hydrothermally brecciated. Another breccia unit occurs here; it is approximately 30 cm thick and consists of jigsaw fragments of hornfels (10 cm in diameter) in a clay matrix.

A granitic inlier occurs within the Burrell Creek Formation approximately 700 m east of Lady Alice North. In hand specimen, it is generally similar to the Allamber Springs Granite. Its presence may be suggestive of a cupola underlying Lady Alice North.

3.2.4 Tabletop Granite

The Tabletop Granite is white/green in colour and is porphyritic. Phenocrysts of orange/pink potassium feldspar (4 mm in diameter) lie within a groundmass of quartz, andesine ($Ab_{35-40}An$), microcline, biotite and hornblende. (Crystals within the groundmass are approximately 3 mm in diameter). Zircons inclusions in biotite are indicated by the presence of uranium haloes. Potassium feldspar phenocrysts are foliated and contain chadacrysts of quartz, hornblende, biotite and potassium feldspar which are less than 1 mm in diameter. Quartz exhibits undulose extinction and is recrystallised at its crystal margins.

The granite-sediment contact crops out approximately 4.3 km north of Pine Creek in several road cuttings along the Stuart Highway. Here the granite is sheared and is juxtaposed against relatively undeformed spotted hornfels. Aplite dykes (0.5 m wide) occur within the spotted hornfels.

3.3 Surficial deposits

Alluvium is found along creeks, rivers and low-lying areas. It consists of angular clasts (5 cm in diameter) of quartz, sandstone greywacke, and siltstone/shale, in a matrix of sandy clay that fines upward on a scale of approximately 1 m. The alluvial horizon is approximately 2 m in thickness and unconformably overlies rocks of the Burrell Creek Formation.

Colluvium occurs on slopes and crests of hills in the prospect. It consists of loose boulders and pebbles of quartz, ferricrete, sandstone greywacke and siltstone/shale.

Hornfels colluvium, quartz and minor granite occurs on ridges to the east of the prospect.

CHAPTER 4

STRUCTURE

4.1 Introduction

At least two phases of deformation have been recognised at the Union Reefs prospect. The earliest deformation (D_1) is characterised by tight folding (F_1), a continuous cleavage (S_1) and mullions. The second deformation (D_2) is characterised by megascopic, long wavelength folds and mesoscopic folds (F_2), a discontinuous spaced and discontinuous crenulation cleavage (S_2), and kinks. D_1 and D_2 correlate with D_3 andD_4 of Johnston (1984), respectively (Section 2.2).

Four quartz vein types are recognised at Union Reefs. Buck quartz and sheeted quartz veins formed during D_1, while breccia zones and quartz sulphide veins formed during D_2.

4.2 First deformation (D_1)

Folds produced during D_1 are north-south trending and plunge to the south. Poles to S_0 indicate the folds plunge 84° toward 189° (Figure 4.1). The folds are tight with a half wavelength of approximately 300-350 m. Axial surfaces are near vertical to steeply westerly dipping, as indicated by apparently thicker beds on the western side of the Broken China Anticline. This asymmetry and the dominant westerly dip of S_0 suggests an eastward tectonic transport direction during D_1. A local plunge reversal is indicated at Lady Alice North from the exposure of fold closure (Figure 4.2) with an average plunge of 24° towards 341° and wallrock fold mullions which plunge 15° toward 350°.

A continuous cleavage (S_1) was observed throughout the prospect as both slaty and phyllitic. The slaty cleavage was well developed in siltstone/shale and the gritstone marker, and to a lesser extent in sandstone greywacke. The phyllitic cleavage was developed in chlorite rich siltstone/shale units.

In thin section, S_1 is defined by the preferred alignment of chlorite and sericite in the wallrock (Figure 4.3). In quartz grains it is defined by a stylolitic to anastomosing foliation parallel to S_1 in the wallrock.

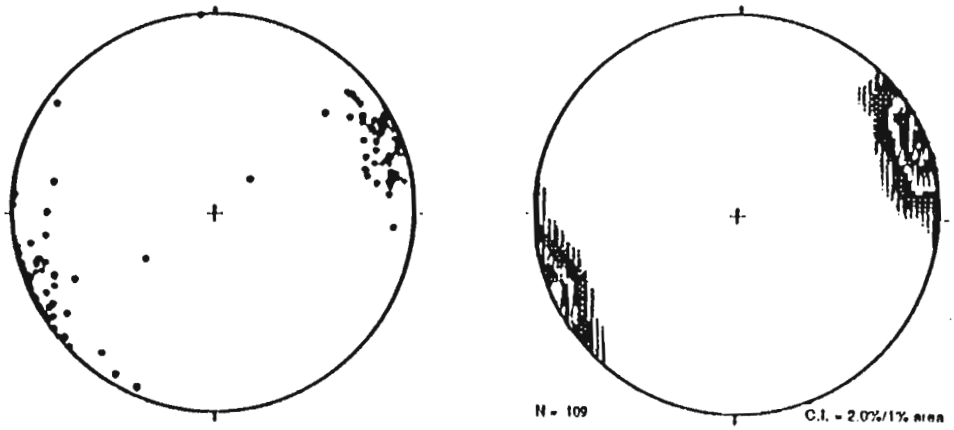

Poles to bedding (S0), trend and plunge of fold axis 189° 84°.

Contoured poles to bedding

Figure 4.1: Equal area stereoplots of poles to bedding (S_0).

The orientation of S_1 is bedding parallel in places, but on average is steeper, and rotated approximately 16° clockwise from bedding; average S_1 is 352° 88° W and average S0 is 336° 83° W. S_1 is steeper than S_0 on both sides of the Broken China Anticline: this is most likely a consequence of shearing. Refraction of S_1 is noted both in outcrop and in the stereonets for S_1 in siltstone/shale and sandstone greywacke (Figure 4.4). Suppe (1985) explained this phenomenon by suggesting that the less competent units take up more of the compression than the more competent units.

Two domains are evident from calculations of S_0 and S_1 intersections. A southerly plunging domain (average plunge of 64° toward 172°) relates to the overall plunge of F_1 folds and northerly plunging domain (average plunge of 64° toward 332°) relates to the local plunge reversal of F_1 folds (Figure 4.5).

Figure 4.2: F_1 fold closure, plunges toward observer (24° toward 341°).

Figure 4.3: Relict cordierite spots in a medium grained siltstone. (Transmitted light-crossed polars).

(i) Spot parallel to the S_1 foliation.

(ii) Spot crosscut by the S_2 foliation.

Figure 4.4: Equal area stereoplots of poles to S_1 cleavage and sketch of S_1 cleavage in outcrop.

4.2

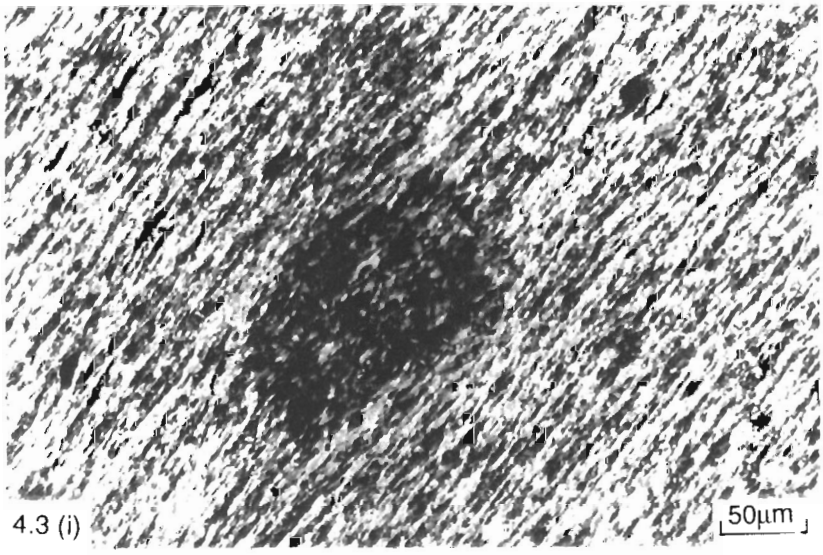

4.3 (i)

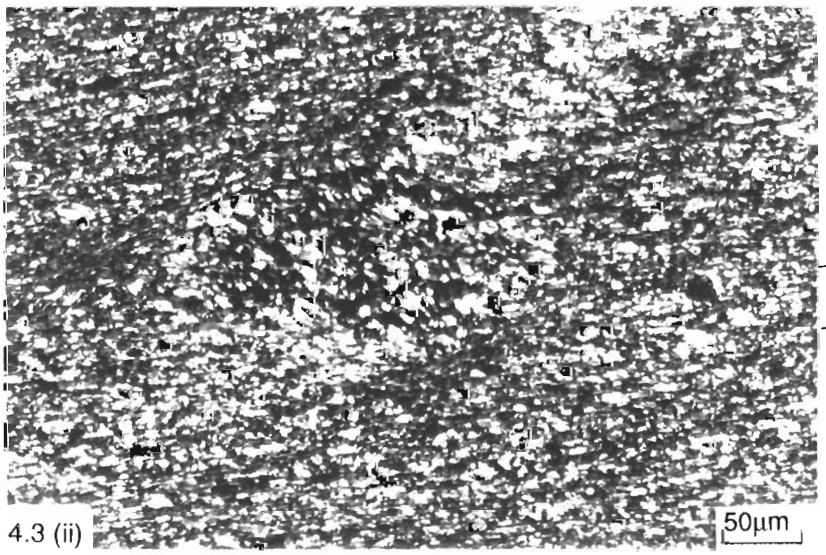

4.3 (ii)

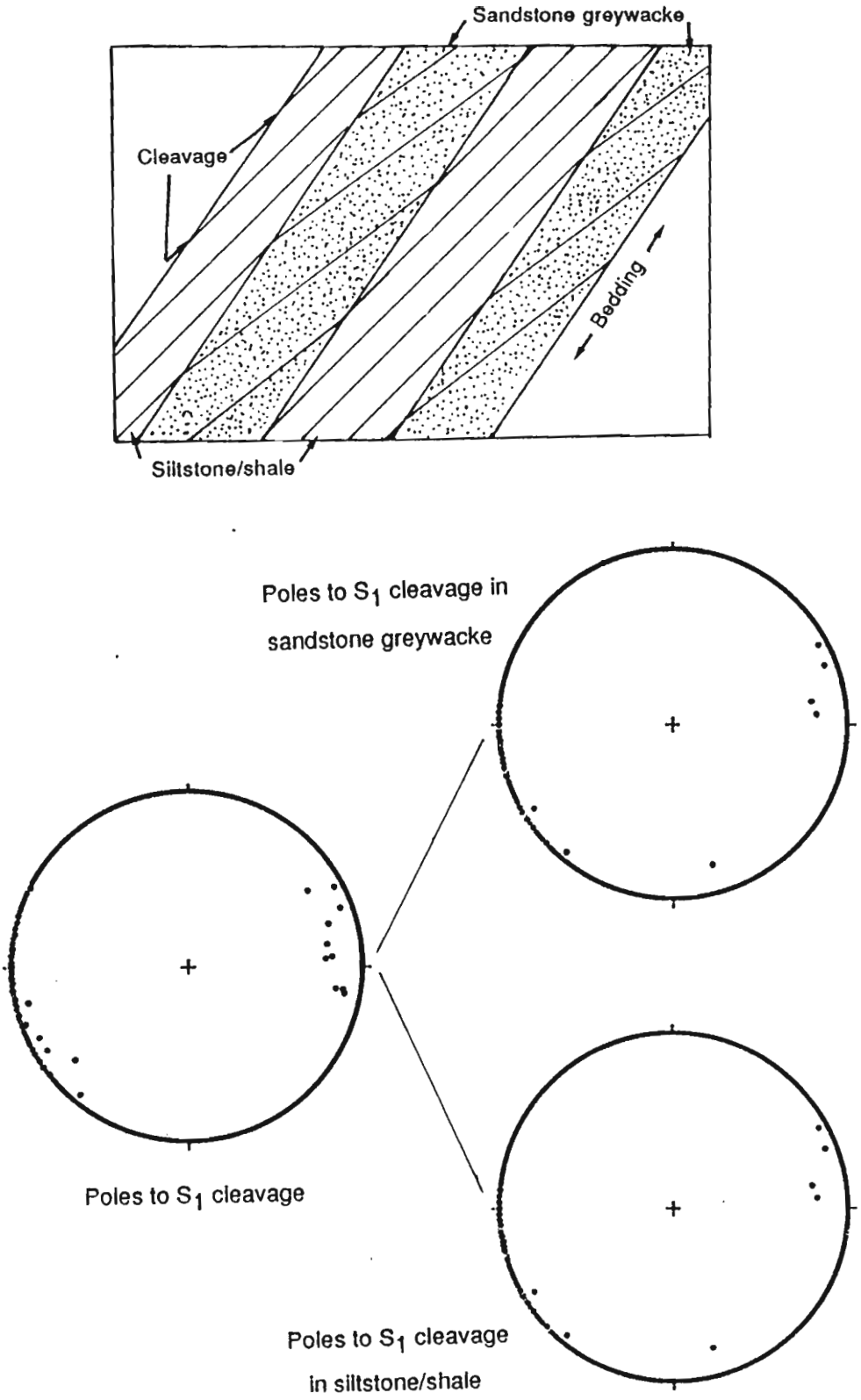

Figure 4.4 Equal area stereolplots of poles to S_1 cleavage and sketch of S_1 cleavage in outcrop.

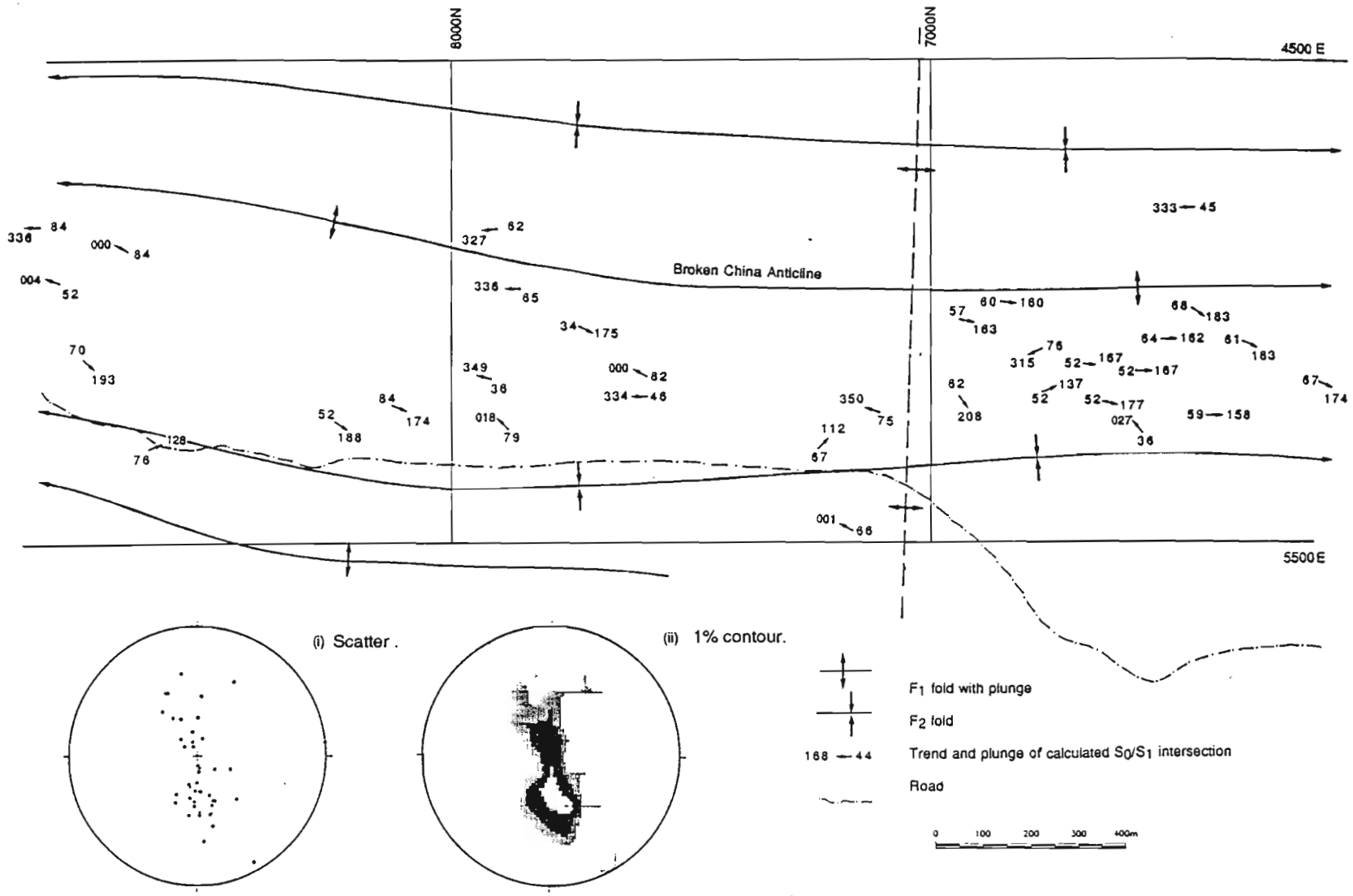

FIGURE 4.5: Sketch and stereonets of S_1/S_0 intersections (calculated).

The north-south trend of F_1 and S_1 indicates that the principal compressive stress (σ_1) would have been directed in an east-west orientation. Shortening involved with this compression is estimated at approximately 55%, as indicated by folded quartz veins.

4.3 Second deformation (D_2)

Megascopic folds produced during D_2 are open and trend east-west with a half wavelength of at least 2 km. A domal structure, produced from the interference of F_2 and F_1, is centred at approximately 7000N 5000E.

Mesoscopic folds produced during D_2 are tight and plunge approximately 70° toward 128° with a half wavelength of less than 1m. They occur within shear zones, where S_1 is folded about the axial planes of mesoscopic F_2 folds. Thel mesoscopic F_2 folds, with a half wavelength of approximately 10-20 cm indicate that shear movement was sinistral on northeast trending structures during D_2.(Figure 4.6).

Two spaced cleavages were produced during D_2, a disjunctive cleavage, observed in sandstone greywacke, and a discrete crenulation cleavage, observed in siltstone shale. The disjunctive cleavage was characterised by parallel fracture like partings approximately 5-10 cm apart, with an average orientation of 306° 87°W.

In thin section the S_2 cleavage is defined by the preferred alignment of individual grains of sericite and quartz (to 25 μm) in the wall rock which overprint the S_1 cleavage (Figure 4.3). In quartz crystal it is defined by fractures parallel to the disjunctive cleavage in the wallrock which overprint the stylolitic to anastomosing foliation in quartz crystals.

The discrete crenulation cleavage (Figure 4.7) was characterised by microfolding of S_1, with the spacing between cleavage domains being in the order of 1.5-2 cm, and the average strike being approximately 193° 90°. Minor offsets, in the order of 1 cm, may occur along this cleavage.

Conjugate kinks were observed north of the Dam; the kink planes strike approximately 280° and 230°. Stubley (1990) suggested that the principal compressive stress (σ_1) is contained within the same dihedral angle between kink planes as the external foliation (thus indicating that σ1 was orientated north-south during D_2.

Figure 4.5: Sketch and stereonets of S_1/S_0 intersections (calculated).

Figure 4.6: F_2 fold in siltstone/shale exhibiting sinistral movement. Compass for scale and orientation.

Figure 4.7: Discrete crenulation cleavage (S_2) developed in siltstone/shale. Compass for scale and orientation.

Figure 4.8: Folded buck quartz vein at Lady Alice North. The axial plane is located in the area in shade. The fold plunges 40° toward 341°. Note the rhombohedral fracture pattern on the eastern limb (note-book side).

4.6

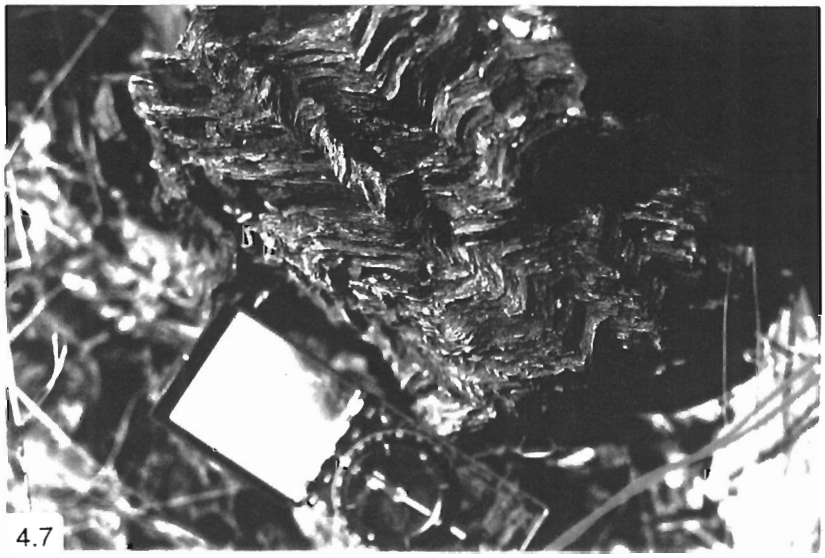

4.7

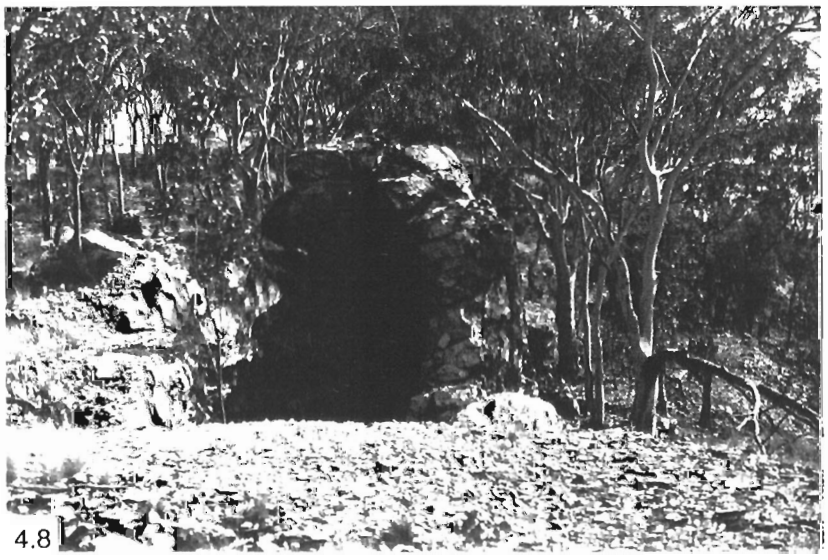

4.8

The east-west trend of D_2 structures and the orientation of conjugate kinks indicate that the principal compressive stress (σ_1) operating during D_2 was orientated approximately north-south. Local shortening involved with this compression is estimated at 52%, as measured from mesoscopic F_2 folding of bedding and quartz veins within shear zones. Regional shortening during D_2 is most likely smaller than this value.

4.4 Quartz veining

4.4.1 Buck quartz veins (V_a)

Massive buck quartz veins are 1-2 m wide (can be as small as 30 cm wide) and consist of milky white, coarse grained, anhedral crystals of quartz. They are commonly bedding parallel and occur within thin (5 m) siltstone/shale units. They occur on the tops of hills and stand proud of the surrounding sediments (up to approximately 2.5 m high). These veins are crosscut by sulphide bearing veins.

At Lady Alice North a 1 m thick vein is folded and plunges 40° toward 341° (Figure 4. 8). It exhibits pinch and swell and a rhombohedral fracture pattern. Mullion structures developed in these veins, plunge approximately 16° toward 328° and reflect the local plunge reversal of F_1 folds.

4.4.2 Sheeted quartz veins (V_b)

Sheeted quartz veins are normally a few cm to 25 cm wide and consist of milky white, medium grained, anhedral crystals of quartz. They predominantly occur in sandstone greywacke units and are crosscut by sulphide bearing quartz. They are associated with crack-seal texture, as defined by Cox and Etheridge (1983).

Sheeted quartz veins may be folded (Figure 4.9) and/or boudinaged. The competency of the host rock controls the orientation of these veins and their thickness, that is to say they are closer to bedding parallel in less competent units than the more competent units. The veins exhibit a foliation which, in cross-section, is observed as a refraction of the S_1 cleavage through the veins. Viewed in long section, the foliation is observed as an anastomosing cleavage termed "crocodile" texture (Figure 4.10).

Figure 4.9: Folded sheeted quartz vein exhibiting shortening (during D_1) of approximately 50 %.. Photograph taken looking north.

Figure 4.10: S_1 foliation in sheeted quartz vein; "crocodile" texture.

Figure 4.11: Quartz sulphide veins in sandstone greywacke. Note the east block up displacement. Photograph taken looking north.

4.9

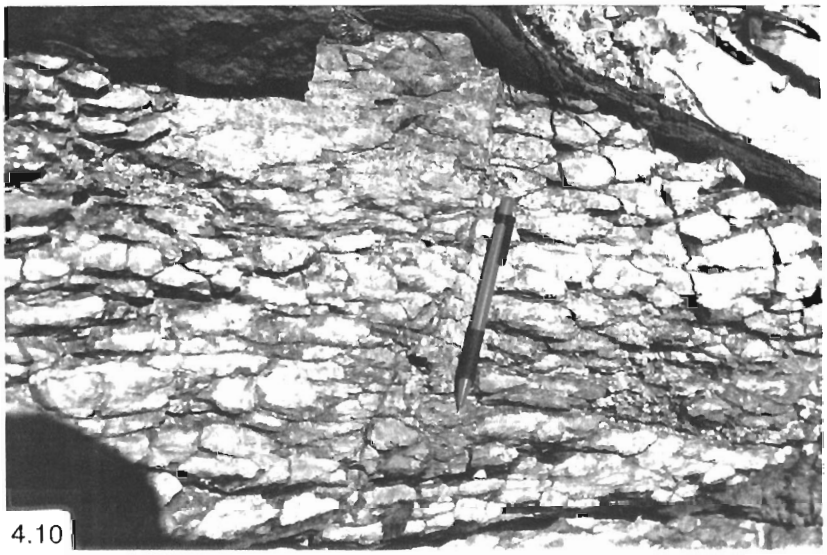

4.10

4.11

4.4.3 Quartz sulphide veins (V_c)

Quartz sulphide veins are a dark red/brown colour. They may show some iron staining and range is size from less than 5 mm to 1-2 cm wide (Figure 4.11). The gossanous nature of these veins suggests a strong association with sulphides. These veins occur as stockworks or as single veins, and crosscut the S_1 cleavage.

4.4.4 Breccia zones (V_d)

Breccia zones measure up to 1 m wide and occur directly at the margins of buck quartz veins, in the vicinity of sheeted quartz veins, and in isolation. They are zones of brecciated quartz, sulphide and country rock which crosscut the S_1 cleavage. They exhibit chloritic and silicic alteration.

4.4.5 Quartz vein formation

Buck quartz veins are folded and exhibit mullion structure indicating they formed prior to D_1. The foliation within, and the folded nature of sheeted quartz veins indicate they also formed prior to D_1.

It is thought that crack-seal texture developed as the first dilational sites began to open up during D_1. Buck quartz and sheeted quartz sulphides veins developed during the early stages of D_1, and were folded by the time of its culmination.

Buck quartz veins formed in the less competent siltstone/shale units, which parted approximately bedding parallel, and allowed a relatively large amount of quartz to be deposited in one site. Sheeted quartz veins formed in competent sandstone greywacke units, which parted in a fracture like manner allowing a relatively limited amount of quartz to be deposited in one site.

The orientation of S_1 during D_2 resulted in dilation and brecciation at the margins of buck quartz veins and areas associated with sheeted quartz veins. Silica/sulphide rich fluids were introduced into these dilatant sites and fractures resulting in the formation of breccia zones and quartz sulphide veins.

4.5 Faulting

4.5.1 Fault/silicified breccia zones

These faults occur as vertical, silicified, resistant zones of brecciated quartz to 2 cm, in a matrix of chlorite, sericite and minor goethite. The quartz exhibits strong undulose extinction and subgrain development.

To the east of Lady Alice North the silicified breccia zones trend 340° and 350°. They are interpreted as faults which were dilated during D_2. The sense of movement on these faults is not known but is possibly dextral, in keeping with movement along northwest trending shear zones during D_2.

Two areas of relatively highly silicified sediment, possibly related to these faults, crop out approximately 200 m east of Lady Alice, and approximately 800 m east of Lady Alice North. They occur as vertical resistant bodies which are orientated approximately perpendicular to the strike of bedding. It is possible that the rocks were silicified by fluids moving along radial fractures formed during the intrusion of the Allamber Springs Granite (K. Hein, *pers. comm.*, 1992).

4.5.2 North-west and north-east striking faults

These faults are dissimilar in both morphology and orientation to fault/silicified breccia zones. The fault zones are filled by fault gouge which ranges in thickness from a few centimetres to half a metre. Where exposed these faults are vertical. Displacement on these faults may have involved a horizontal and vertical component.

A lineament analyses of these faults has resolved three prominent strike orientation; (i) 280°-290°, (ii) 310°-320° and (iii) 010°-030° (Figure 4.12). Fault groups (i) and (ii), which strike aaproximately north-west, are locally dominant.

Offset on these faults is both dextral and sinistral. This may be explained by invoking a non-coaxial sinistral stress field during D_1 and a non-coaxial dextral stress field during D_2, and ascribing fault strike to the stress field shear orientations (Figure 4.13). During D_1, group (i) corresponded to sinistral R_1 shears, while

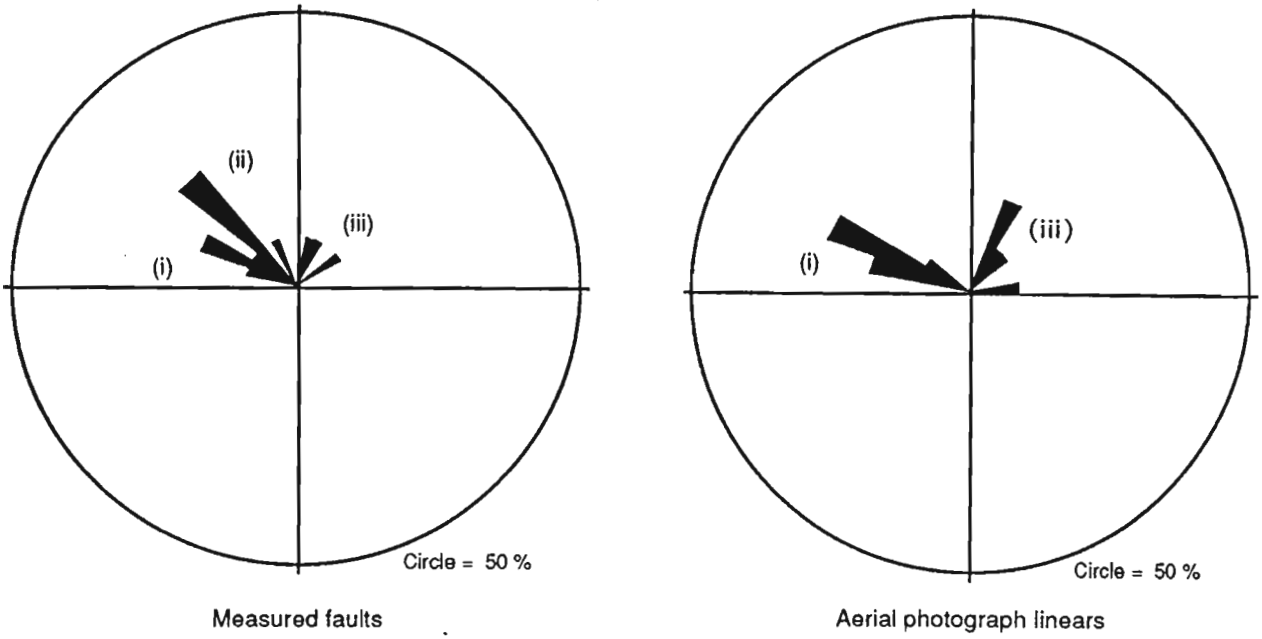

Figure 4.12: Rose diagram of measured faults and aerial photoograph linears; group (i) are west-northwest trending faults, group (ii) are northwest trending faults, and group (iii) are northeast trending faults.

during D_2, group (i) corresponded to dextral P shears. Similarly group (ii) corresponded to sinistral P shears during D_1, and to dextral R_1 shears during D_2. Group (iii) corresponded to dextral X shears during D_1 and to sinistral R_2 shears during D_2. D_1 X shears, or D_2 R_2 shears, were not identified in this study. Furthermore, faults active during D_1 may not have been active during D_2.

4.5.3 Shear zones and north-south striking faults

Shear zones are characterised by large variations in the dip and strike of S_0 and S_1, and the presence of mesoscopic F_2 folds. F_2 folding was chaotic in the more intense sections of the shear zones. The zones predominantly occur in siltstone/shale units and also in close proximity to fold hinges, such as at Lady Alice North and Millars. This suggests that the shear zones have exploited the weaker lithological zones. Movement is sinistral east-block-up and oblique, as indicated by offset along shear planes slickenslides, the sigmoidal shape of shear zones, mesoscopic F_2 folds, and drag on bedding.

North-south striking faults are vertical and close to bedding parallel. On the western side of the Broken China Anticline they display east-block-up movement, while to the east of the Broken China Anticline they display east-block-down movement. This indicates that the block bounded between these two north-south striking fault groups has been uplifted.

4.6 Structural controls on mineralisation

Figure 1.3 and the cross-sections on Figure 4.14 illustrate the features outlined in this section.

The bulk of mineralisation at the Union Reefs prospect is located on the western limb of the Broken China Anticline. Some zones of mineralisation are located on the hinge zone of the Anticline, such as at Lady Alice North and Ping Ques'.

In regard to the domal structure produced by the interference of F_2 and F_3 folds, the bulk of the mineralisation (i.e., Union Central, Crosscourse and Ping Ques') is located on the southern, southerly plunging portion of the dome. Mineralisation at Union North and Lady Alice North occurs on the northern, northerly plunging portion of the dome. Since there is insufficient evidence to suggest a southerly plunge to the mineralisation in the south of the dome, or to suggest a northerly plunge to mineralisation in the north of the dome, it can not be concluded that the mineralised body was domal in form. However, this does not preclude the possibility that the domal structure had some overall control on location of the sites of mineralisation.

Mineralised bodies have a strong association with fault bounded blocks and corridors, ie., corridors which are bounded by north-west striking faults, and blocks bounded by northwest and northeast striking faults and /or northwest and north striking faults. For example:-

1. At Union Central, Crosscourse, Ping Ques' and Union North, the bulk of the mineralisation is contained within a corridor, approximately 700 m wide, bounded by two north-westerly trending faults.

2. At Union North the zone of mineralisation is located within a corridor approximately 425 m wide.

3. At Lady Alice and Lady Alice North mineralisation is located within blocks created by the intersection of north-easterly and north-westerly trending faults.

It is speculated that the corridors and blocks have been uplifted during D_2 (ie. σ_1 orientated north-south and σ_3 orientated east-west) causing east-west dilation within

7900N SECTION

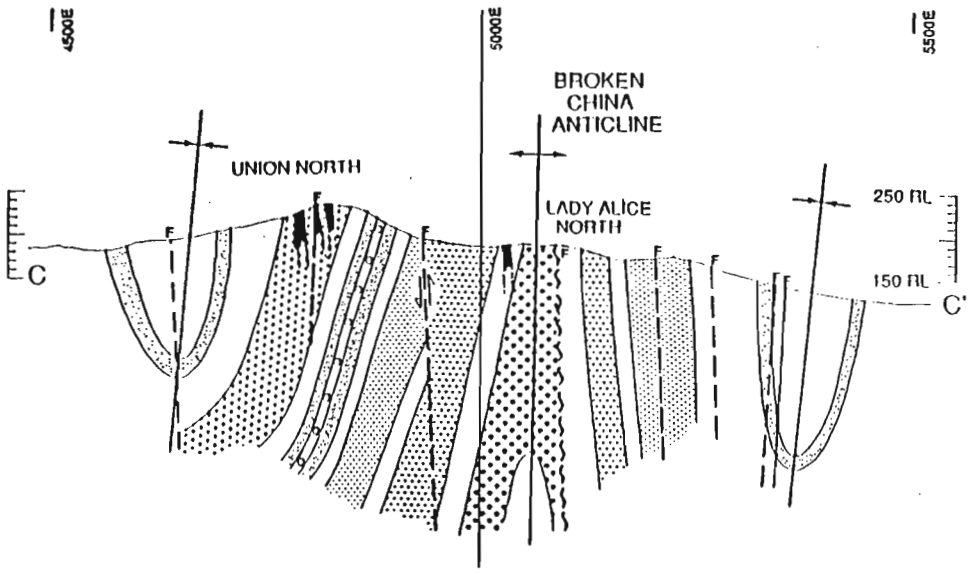

6690N SECTION

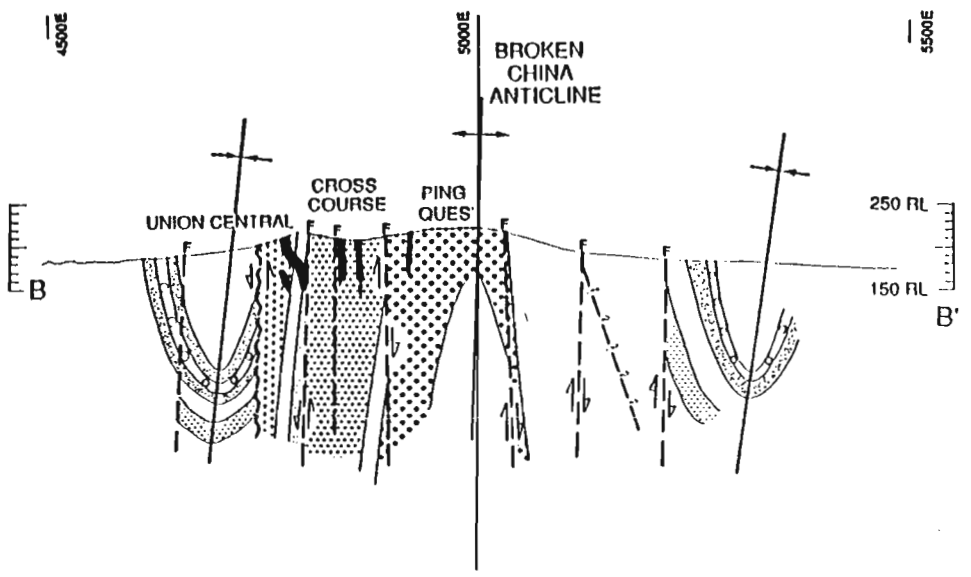

6490N SECTION

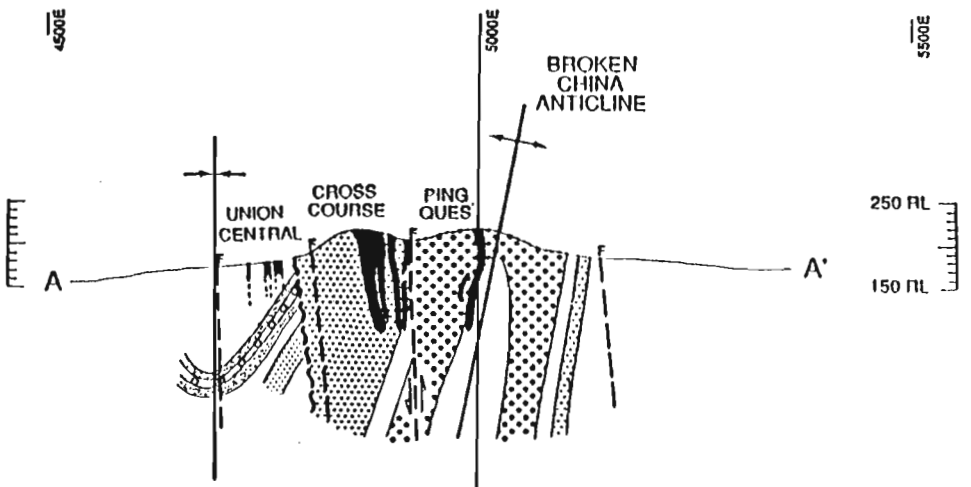

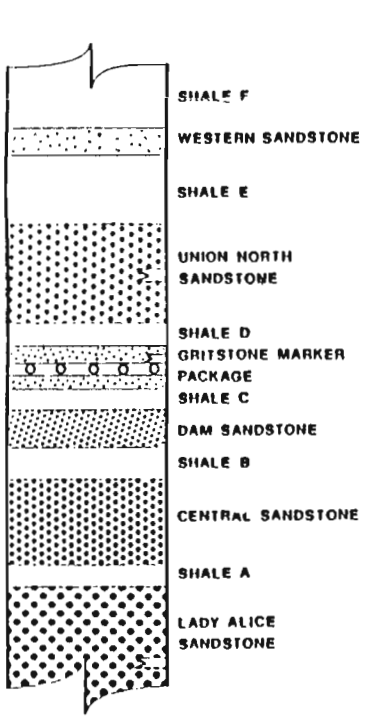

STRATIGRAPHIC COLUMN
UNION REEFS, N.T.

LEGEND

- Fault
- Anticline
- Syncline
- Gritstone marker
- Surface projection of mineralisation

0 100 200 300 400m

Billiton Australia
The Metals Division of the Shell Company of Australia Limited

Project
UNION REEFS PROJECT
NORTHERN TERRITORY

Title
Cross-sections AA', BB' and CC'.

Author J.S.D.	Office	Scale	
Drawn	Date	Revised	Date
Plotted date		Report No.	
Drawing No.		Fig. No. 4.14	

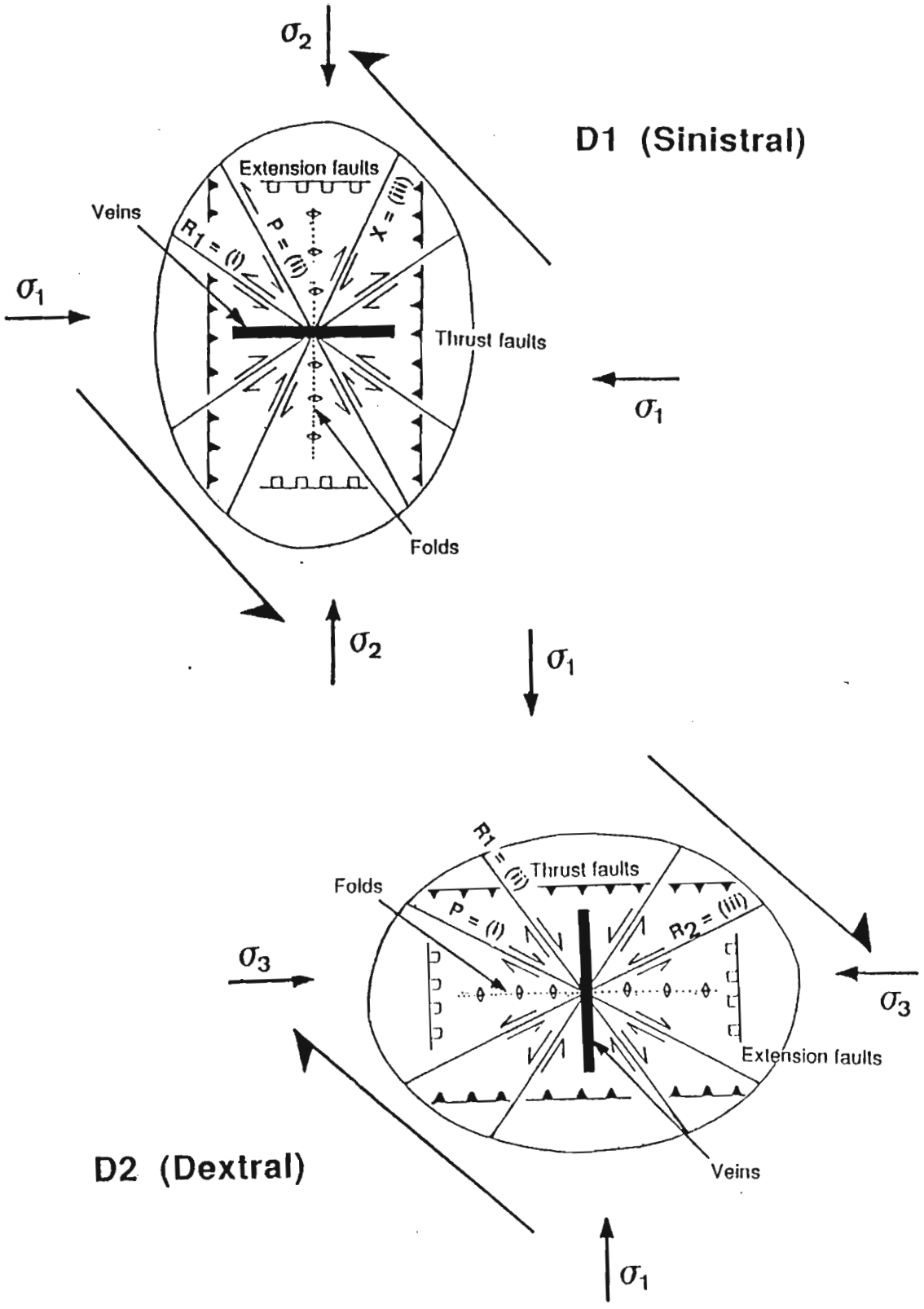

FIGURE 4.13: Non-coaxial stress field diagrams; D_1 sinistral, D_2 dextral. Group (i) are west-northwest trending faults, group (ii) are north-west trending faults and group (iii) are north-east trending faults.

the corridors and blocks. The synchronous uplift and dilation, accompanied by a pressure decrease, may have created north-south trending fractures, thus allowing mineralising fluids to focus. The sub-block (approximately 225 m wide) containing Cross Course, Ping Ques and Union Central probably suffered the greatest dilation and/or uplift.

The relationship between shear zones and mineralisation suggests that shear zones are not favourable hosts to mineralisation. This is indicated at Union Central where a mineralised body crosscuts a shear zone. Since σ_1 during D_2 would have been orientated parallel to the strike length of the mineralised bodies, and since the shear zones in the region are sub-parallel to σ_1, it is suggested that they were in an unfavourable orientation with respect to dilation.

At the Union Reefs prospect, there is a structural control on the sites of mineralisation which is lithologically dependent. That is, the bulk of the mineralisation is hosted in the Lady Alice Sandstone, the Central Sandstone and the Union North Sandstone. The predominant occurrence of mineralisation within these competent stratigraphic units is probably a consequence of fracturing, in that competent lithologies preferentially fracture under strain, while less competent units develop bedding parallel faults, shear or part. The occurrence of mineralised zones within siltstone/shale units does not however, preclude their potential to host mineralisation. Indeed, minor mineralised zones are located within siltstone/shale units at Lady Alice North, Union North and Union Central.

4.8 Metamorphism

4.7.1 Introduction

The sediments (Burrell Creek Formation) at the Union Reefs prospect show evidence that they have been subjected to two metamorphic events. The first event involved greenschist facies metamorphism and was associated with low grade regional metamorphism during the Top End Orogeny. The second event occurred during intrusion of granitoids of the Cullen Batholith and resulted in contact metamorphism ranging in grade from the hornblende-hornfels facies to the albite-epidote facies.

4.7.2 Regional metamorphism

The Union Reefs prospect lies within the low grade regional metamorphic province II of the Pine Creek Inlier, as defined by Ferguson (1980). At the prospect, greenschist facies metamorphism developed in the mineral assemblage: quartz-iron oxides-chlorite-sericite-biotite. Chlorite and sericite have a preferred orientation parallel to a slaty cleavage (S_1) produced during the earliest deformation (D_1), indicating that this deformation event was approximately synchronous with regional metamorphism.

4.7.3 Contact metamorphism

In the Pine Creek area, Stuart-Smith *et al.* (1987) defined a 2 km wide contact aureole adjacent to the Cullen Batholith, which overprinted regionally metamorphosed sediments of the Burrell Creek Formation. The aureole consisted of an outer albite-epidote hornfels facies zone with a narrower, inner hornblende hornfels facies zone.

At the Union Reefs prospect the contact aureole of the Allamber Springs Granite extends approximately 1.5 km from the granite-sediment contact (Figure 1.3). The contact aureole of the McMinns Bluff Granite and the Tabletop Granite do not impinge on the prospect.

The limit of hornblende-hornfels facies alteration is equivalent to the contact aureole of the Allamber Springs Granite and is characterised by the mineral assemblage: quartz-biotite-cordierite-hornblende-iron oxides. The extent of the contact aureole was defined by the presence, or lack of, relict cordierite spots in hand specimen. The spots are black in colour and range in size according to their position within the contact aureole. In sediments at the distal margin of the contact aureole, the spots are spherical and approximately 3 mm in diameter. In sediments proximal to the sediment-granite contact, spots are located within a shear zone and are elongate (12 x 5 mm in size) parallel to the granite-sediment contact.

Relict cordierite spots observed in thin section of drill core are characterised by the presence of sericite, chlorite and an enrichment in quartz relative to the surrounding sediment. They are elongated (1 x 0.2 mm) parallel to the S_1 foliation and are crosscut by the S_2 foliation (Figure 4.3). These spots formed prior to D_1, possibly due to the contact metamorphic effects of the Bludells Monzonite.

Mineralisation at the Union Reefs prospect is located close to the distal margin of the contact aureole of the Allamber Springs Granite. Most mineralised zones within the prospect are located within approximately 350 m of this margin (Figure 1.3).

4.7.4 Conditions of metamorphism

Ferguson (1980) stated that the pressure and temperature regime that produced greenschist facies metamorphic rocks was less than 4 kb and 400-500°C (Figure 4.15). The upper pressure limit was indicated by the absence of almandine, while the lower and upper temperature limits are indicated by the presence of biotite and the absence of cordierite, respectively.

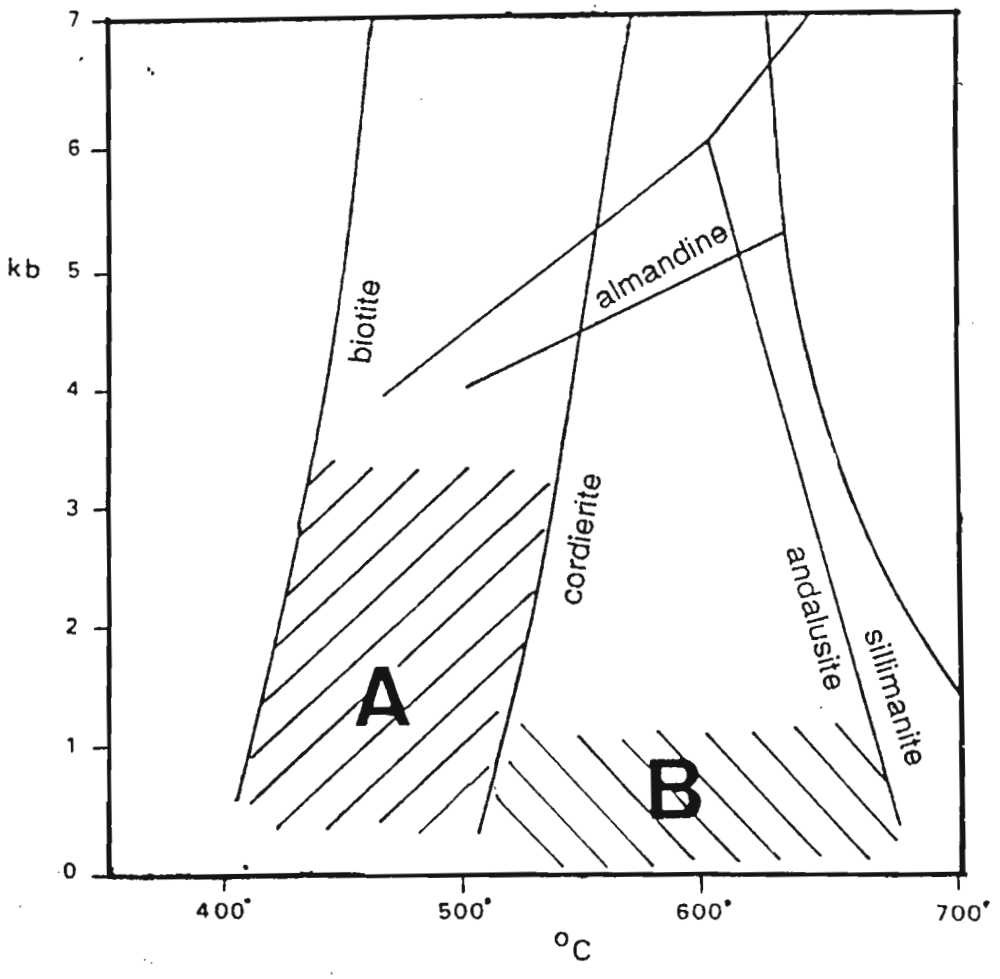

FIGURE 4.15: Pressure-temperature diagram showing the approximate fields of regional (Regime A) and contact (Regime B) metamorphism. Modified after Ferguson (1980, Figure 5, pp. 97).

He added that the pressure and temperature regime that produced contact metamorphism was less than 2.5 kb and 500-680°C (Figure 4.15). The upper pressure limit was indicated by the presence of andalusite and the absence of sillimanite. The lower temperature limit was indicated by the presence of cordierite and the upper temperature limit was indicated by the absence of sillimanite and the presence of andalusite.

4.7 Structural history

During D1 the maximum compressive stress (σ_1) was orientated east-west and the minimum compressive stress (σ_3) was vertical. It is likely that a non-coaxial sinistral stress field operated during D_1, with sinistral movement on north-west trending faults (R_1 and P shears) and dextral movement on north-easterly trending faults (X shears). The formation of buck quartz and sheeted quartz veins occurred early in D_1. These veins were folded subsequent to their formation and a stylolitic to anastomosing foliation (S_1) developed within them at the culmination of D_1. The sediments were tightly folded and a continuous slaty cleavage (S_1) developed in them at the culmination of D_1. The sediments were subjected to regional metamorphism to greenschist facies during D_1.

During D_2, the maximum compressive stress (σ_1) was orientated north-south and the minimum compressive stress (σ_3) was orientated east-west. It is likely that a non-coaxial dextral stress field operated during D_2, with dextral movement on north-west trending faults (P and R_1 shears) and sinistral movement on north-easterly trending faults (R_2 shears). The formation of breccia zones and quartz sulphide veins occurred early in D_2 when dilatant structures were formed within uplifted, fault bounded blocks and corridors. Long wavelength folds, mesoscopic folds, a discontinuous spaced and crenulation cleavage, and conjugate kinks were produced in the sediments at the culmination of D_2. The S_1 cleavage was folded by F_2 folds.

CHAPTER 5

MINERALISATION

5.1 Introduction

Mineralisation at the Union Reefs prospect is associated with breccia zones and quartz sulphide veins, and crosscuts buck quartz veins and sheeted quartz veins. Gold mineralisation is associated with arsenopyrite, bismuth, bismuthinite and an unidentified phase. Other sulphide minerals present include pyrrhotite, marcasite, pyrite, sphalerite, chalcopyrite and galena. Gangue mineralogy consists of quartz, chlorite, sericite and calcite.

5.2 Mineralisation textures

The principal sulphide mineral is arsenopyrite. It occurs as subhedral to anhedral grains to 20 mm which are brecciated and/or boudinaged. It occurs as fill in fractures within anhedral quartz, and overprints and consumes pyrrhotite.

Pyrrhotite occurs as brecciated spongy anhedra to 20 mm. It occurs as fill within fractures in anhedral quartz and within anhedral arsenopyrite (to 0.01 mm). This indicates that pyrrhotite precipitation preceded that of arsenopyrite and crystalline marcasite. Pyrrhotite is commonly altered to supergene marcasite and pyrite (birdseye texture), the alteration being crystallographically controlled by cleavage planes of the pyrrhotite (Ixer, 1991).

Pyrite and lath-shaped marcasite occurs as brecciated euhedral to subhedral grains to 20 mm. The occurrence of pyrite within euhedral marcasite is as common as marcasite within euhedral pyrite, and crosscutting relationships have not been observed. This suggests that pyrite and marcasite precipitated at about the same time. Since marcasite/pyrite precipitation is pH dependent (marcasite precipitation below pH of 4.5 and pyrite precipitation above pH of 4.5), it is possible the FeS_2 precipitation occurred during fluctuations in pH (Schoonen & Barnes, 1991). The sulphides occur as fill within fractures in arsenopyrite (Figure 5.1), pyrrhotite and anhedral quartz, indicating that marcasite and pyrite precipitation postdated that of arsenopyrite, pyrrhotite and quartz.

Figure 5.1: Pyrite (py) within fractures in arsenopyrite (ars). Note the brecciated nature of the sulphides. (Reflected light).

Figure 5.2: (i) and (ii): "Dusting" and "watermelon" chalcopyrite disease in sphalerite. Note the chalcopyrite (black in 5.2(i)) within fractures and cleavage planes in honey coloured sphalerite. ((i) Transmitted light, (ii) reflected light).

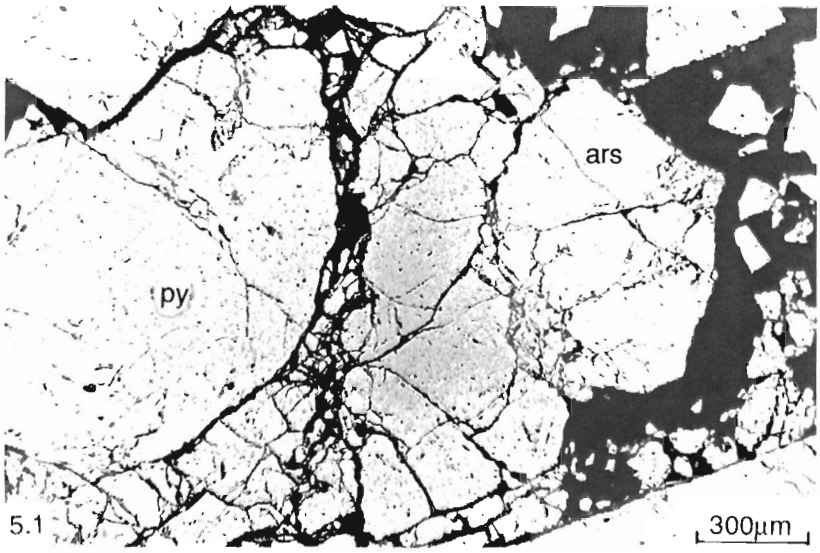

5.1

5.2 (i)

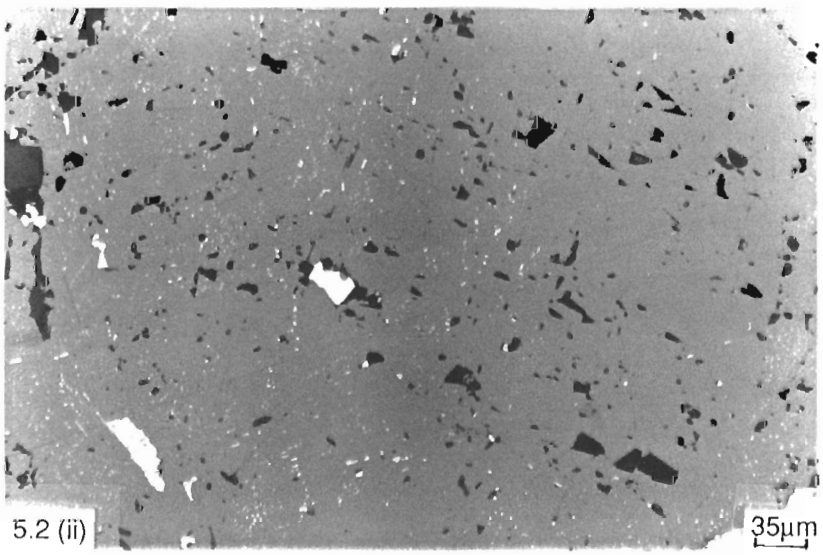

5.2 (ii)

Sphalerite occurs as anhedral grains to 20 mm, averaging approximately 1 mm. It is generally associated with chalcopyrite, the association being suggestive of chalcopyrite disease, in particular, "dusting" and "watermelon" texture (Figure 5.2 (i) and (ii)) (Barton & Bethke, 1987). The texture is the result of the replacement of Fe-rich sphalerite by chalcopyrite and Fe-poor sphalerite as an integral part of the mineralisation process, and indicates a moderate temperature (200-400°C) of sphalerite precipitation (Barton & Bethke, 1987). Chalcopyrite occurs along fractures within the sphalerite indicating that the sphalerite was brecciated prior to, and during, the onset of disease. Chalcopyrite also occurs along sphalerite cleavage planes. Sphalerite occurs as fill within fractures in arsenopyrite, pyrrhotite, crystalline marcasite and quartz. Sphalerite is commonly altered to supergene marcasite (birdseye texture), the alteration being crystallographically controlled by cleavage planes of the sphalerite (Ixer, 1991).

Chalcopyrite occurs as spongy anhedral grains to 10 mm, and as massive veins approximately 3 cm wide. It occurs in contact with pyrrhotite and as fill to fractures in arsenopyrite, pyrrhotite, sphalerite and anhedral quartz. Occasionally, chalcopyrite is seen to share smooth curved boundaries with sphalerite, suggesting that chalcopyrite precipitation was, in part, synchronous with that of sphalerite. This is consistent with observations of chalcopyrite disease in sphalerite. Chalcopyrite in fractures in pyrrhotite and arsenopyrite probably precipitated at this time. Early precipitation of chalcopyrite in equilibrium with pyrrhotite, is indicated by the presence of smooth curved or embayed margins between the two sulphides.

Gold exhibits a bright yellow colour and ranges in size from 25 μm to 1 mm. Gold and bismuthinite (average size 0.03 mm) display smooth curved margins where in contact, suggesting that they were precipitated at the same time (Figure 5.3). Gold occurs as fill within fractures in brecciated arsenopyrite grains (Figure 5.4), and as fill in fractures in anhedral quartz (usually within 0.02 mm of the arsenopyrite grains). Bismuthinite occurs in fractures within arsenopyrite and sphalerite, indicating that precipitation of gold and bismuthinite was late.

The presence of rare anhedral bismuth (average size 0.03 mm) within fractures in quartz may suggest that bismuth was co-precipitate with gold and bismuthinite, especially since bismuth is frequently associated with bismuthinite in mineral deposits (Ramdohr, 1980).

Figure 5.3: Gold (Au) and bismuthinite (bis) in a fracture in arsenopyrite (ars). Note the regular nature of the contact between the bismuthinite and the gold. (Reflected light).

Figure 5.4: Gold (Au) within fractured arsenopyrite (ars). The fractures in the arsenopyrite are parallel to the S_2 foliation. (Reflected light).

Figure 5.5: Bismuthinite (bis) and an unknown phase (unk) in fractures in quartz (q) and arsenopyrite (ars). (Reflected light).

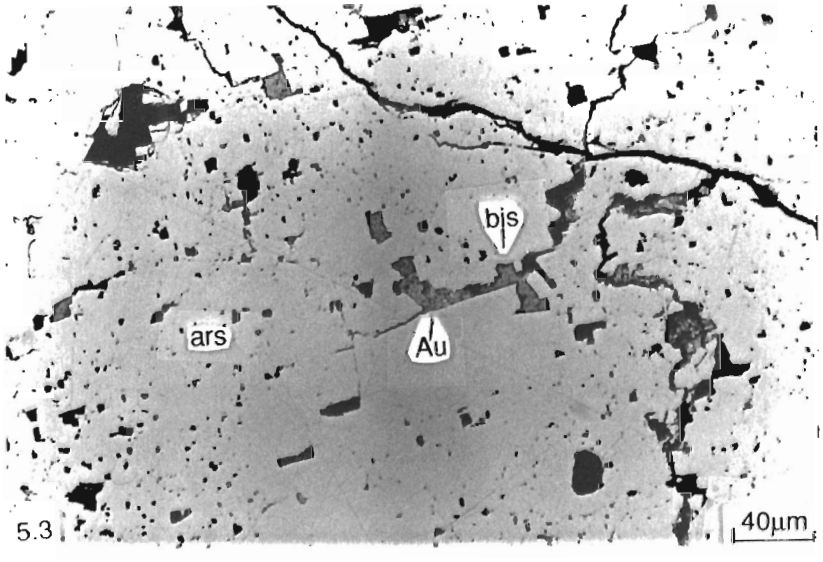
bis
ars
Au
5.3
40µm

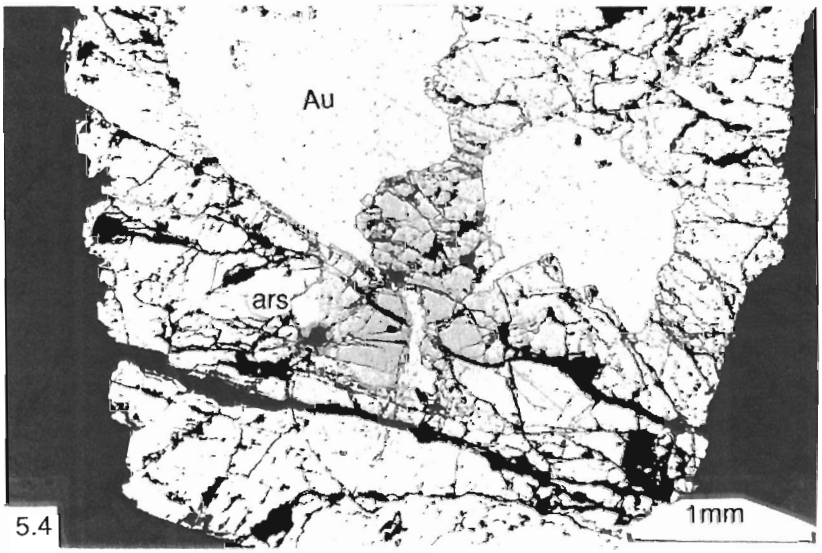
Au
ars
5.4
1mm

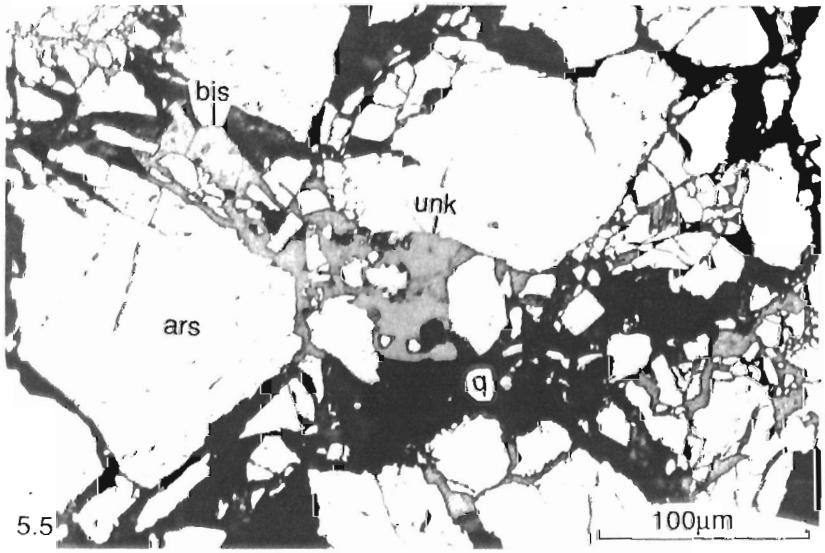
bis
unk
ars
q
5.5
100µm

An unidentified greenish yellow anhedral mineral (to 100 μm) shares smooth curved and embayed margins with bismuthinite, suggesting that bismuthinite and this mineral precipitated in equilibrium (Figure 5.5). The unknown mineral also occurs as fill to fractures in arsenopyrite. It has similar optical properties to chalcopyrite, but is distinguished by its slightly greater hardness and greenish tinge in reflected light . It is similar in habit and general optical properties to the mineral talnakite ($Cu_9Fe_8S_{16}$) which occurs in Au prospects in the Mt Todd district in equilibrium with bismuth, bismuthinite and gold (K. Hein, *pers. comm.*, 1992).

Galena occurs as anhedral deformed grains with an average size less than 1 mm (Figure 5.6). It occurs as fill within fractures in pyrrhotite, marcasite, sphalerite and chalcopyrite, indicating that it precipitated after those sulphides. The relationship of galena to gold, bismuth, bismuthinite and the unidentified phase has not been established. However, it is suggested that galena formed prior to the precipitation of these minerals, in keeping with generally accepted metal zonation models (Large, 1991). Sigmoidal polish pit trails on the polished surface indicate that the galena was deformed after its emplacement.

Euhedral to subhedral arsenopyrite, pyrrhotite, marcasite, pyrite, sphalerite and chalcopyrite also occur within the alteration selvedge adjacent to sulphide bearing quartz veins. They are generally finer than those sulphides within quartz veins (to 10 mm) and occur as "train" like groups which lie parallel to, and overprint, the S_1 foliation. This suggests that the sulphides were precipitated after the foliation had developed, ie., post D_1.

5.3 Gangue mineralogy

The principal gangue mineral is quartz. Early quartz occurs as 0.01 mm to 40 mm sized crystals which exhibit crack-seal texture (Figure 5.7), and which display strong undulose extinction. Crystal boundaries are irregular and concavo-convex to stylolitic. Internally, the crystal exhibits a stylolitic to anastomosing foliation, approximately parallel to S_1 in the wallrock. Clearly, the vein must have formed prior to the fabric.

Late quartz is associated with fracture-like trails (to 0.05 mm wide) that are related to recrystallisation of early quartz during the development of an S_2 foliation.

Figure 5.6: Deformed galena (gn) within fractures in sphalerite (sph). (Reflected light).

Figure 5.7: Crack-seal texture in quartz. Crystal boundaries are irregular and concavo-convex to stylolitic. Wallrock lies on the right hand side of the photograph (black). (Transmitted light-crossed polars).

Figure 5.8: Paragenetic sequence for gold mineralisation in the Union Reefs prospect.

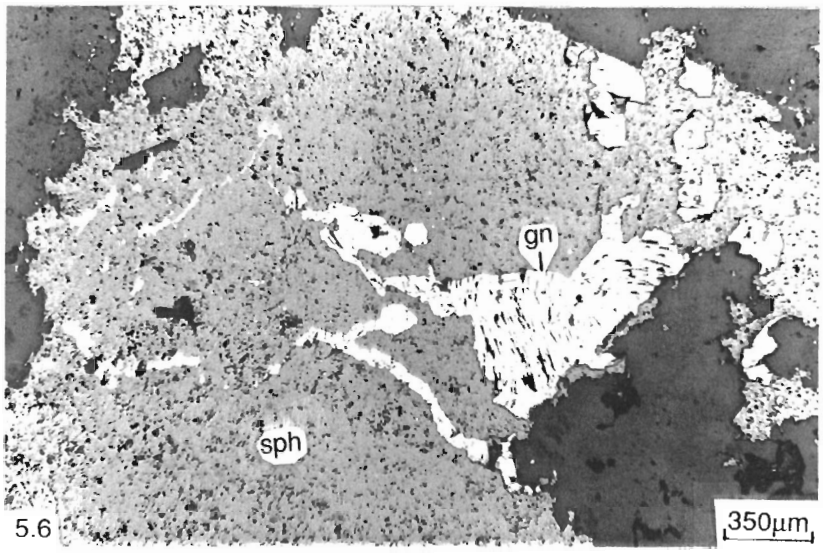
gn
sph
5.6
350µm

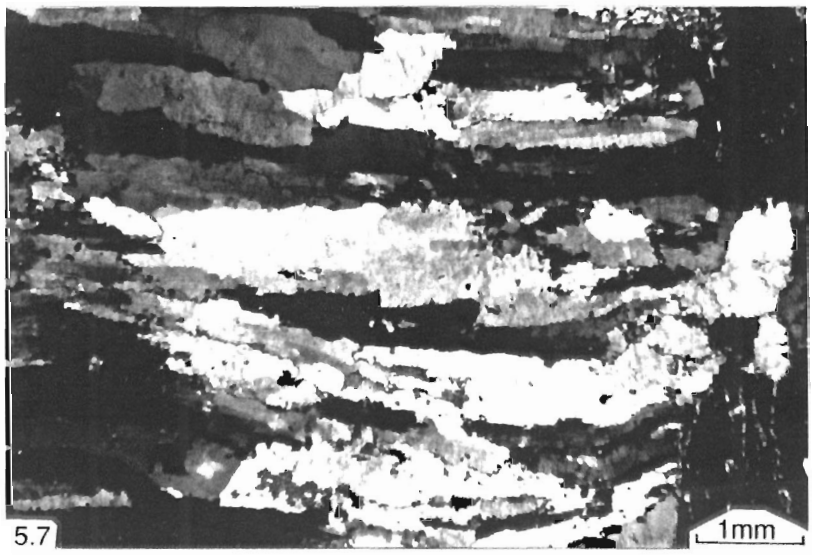
5.7
1mm

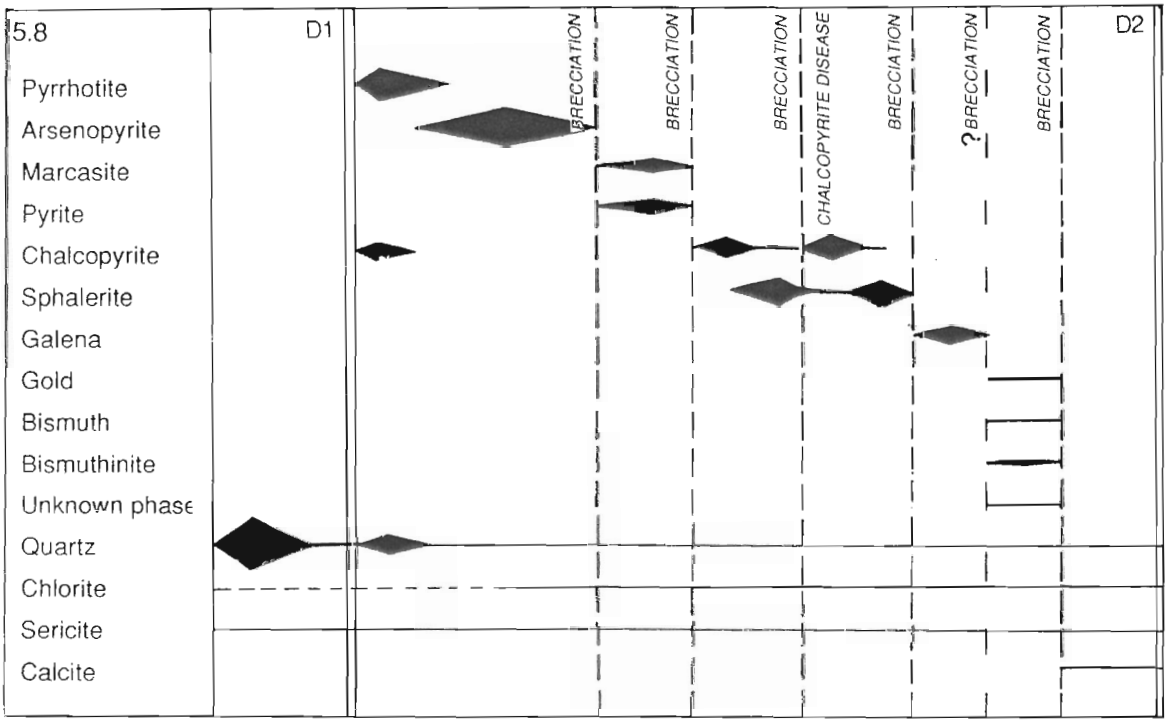
5.8
D1
BRECCIATION
BRECCIATION
BRECCIATION
CHALCOPYRITE DISEASE
BRECCIATION
?BRECCIATION
BRECCIATION
D2
Pyrrhotite
Arsenopyrite
Marcasite
Pyrite
Chalcopyrite
Sphalerite
Galena
Gold
Bismuth
Bismuthinite
Unknown phase
Quartz
Chlorite
Sericite
Calcite

The quartz is fine grained and exhibits a granoblastic texture. The parallel to sub-parallel trails containing this quartz, crosscut arsenopyrite boudins and the S_1 foliation. Granoblastic quartz, between arsenopyrite boudins, were probably formed during development of the S_2 foliation.

From the above, it can be establisehed that quartz precipitation occurred prior to, and during, the formation of the S_1 stylolitic to anastomosing foliation, and prior to and during, the formation of the granoblastic S_2 foliation.

Alteration selvedges associated with quartz veins are not common. However, where observed, they extend up to 0.4 mm into the wallrock from the vein edge and are characterised by the predominant development of chlorite.

Chlorite is associated, but not exclusively, with sericite in both the wallrock and quartz veins. It occurs in fractures within arsenopyrite, pyrrhotite, marcasite, sphalerite, chalcopyrite, galena and quartz. Chlorite occurs as laths (0.01 mm) and/ or fan shaped aggregates, while sericite occurs as laths (0.01 mm).

Brecciated calcite grains to 0.1 mm, fill within fractures in arsenopyrite, pyrrhotite, marcasite, sphalerite, chalcopyrite, galena and quartz, and overprint chlorite, sericite and bismuth. This suggests that calcite precipitated in the final stage of the mineralisation event.

5.4 Deformation textures

From the above description, it is apparent that sulphide precipitation postdated the development of the S_1 foliation and preceded the development of the S_2 foliation. Arsenopyrite anhedra overprint the S_1 cleavage in quartz sulphide veins, and all sulphides overprint, and lie parallel to, the S_1 cleavage in the wallrock. Arsenopyrite is crosscut by the S_2 granoblastic foliation and was probably boudinaged during the formation of this fabric. Galena was probably micro-folded at this time. The main fracture orientation within sulphides lies parallel to the S_2 cleavage within the wallrock, and parallel to fractures within the quartz which crosscut the S_1 foliation

5.5 Paragenesis

From the textural relationships above, a paragenetic sequence can be established as follows (Figure 5.8):-

1. Pyrrhotite and chalcopyrite were co-precipitate.
2. Precipitation of arsenopyrite followed and was terminated by a brecciation event.
3. Marcasite and pyrite were formed during fluctuation in pH, prior to a brecciation event.
4. Chalcopyrite precipitation was followed by that of sphalerite.
5. A brecciation event preceded the replacement of iron-bearing sphalerite by chalcopyrite and low-iron sphalerite during "dusting" and "watermelon" chalcopyrite disease.
6. Precipitation of sphalerite continued subsequent to chalcopyrite disease, but was interrupted by a brecciation event.
7. Precipitation of galena followed that of sphalerite, but was interrupted by a brecciation event.
8. Precipitation of gold, bismuth, bismuthinite, and the unidentified phase.

In terms of gangue mineralogy, quartz, chlorite and sericite precipitation was probably continuous. Calcite was the final mineral precipitated and was subsequently brecciated.

CHAPTER 6

SULPHUR ISOTOPES

6.1 Introduction

Sulphur isotopes can provide information on the temperature of mineral deposition, the source of mineralising fluids, the chemical environment of mineral deposition, and the potential for fluid mixing processes. This Chapter uses sulphur isotope abundances to constrain one or more of these aspects.

Sulphur isotope ratios were measured on 14 pyrite, 7 arsenopyrite, 5 pyrrhotite, 3 sphalerite and 1 chalcopyrite sample (30 in total). $\delta^{34}S$ values for pyrite, arsenopyrite, pyrrhotite and sphalerite range from 4.7‰ to 9.5 ‰, with an average of 6.6‰ (Figure 6.1 and Table 6.1).

The average $\delta^{34}S$ value for the chalcopyrite sample is 11.6‰, almost twice the value for the other sulphides. Petrographically the sample from which the value was obtained precipitated at approximately the same time as sphalerite. With this in mind this value must be considered uninterpretable.

6.2 Geothermometry and isotopic equilibrium

Estimation of temperature of mineralisation using sulphide pairs as geothermometers, as described by Ohmoto and Rye (1979), produced geologically unreasonable temperatures. Calculations using $\delta^{34}S$ values for co-existing pyrite and pyrrhotite gave a temperature of approximately 2180°C (this value was calculated by taking $\delta^{34}S$ to two decimal places) and 310°C. These results must be considered meaningless given the variation between them.

Sulphur isotope geothermometry is based on temperature dependent isotopic equilibrium fractionation between different sulphide species. In this case precipitation of pyrite and pyrrhotite may have been relatively rapid, with no time for sulphur to fractionate between them and obtain isotopic equilibrium.

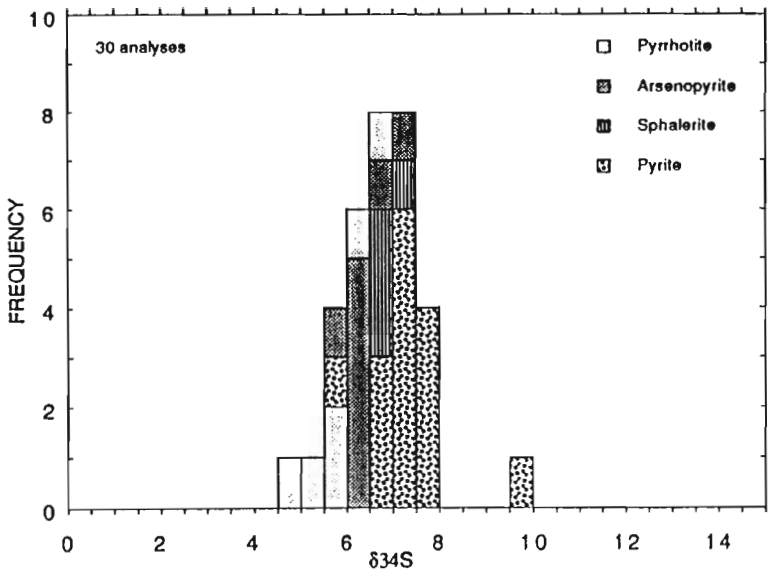

FIGURE 6.1: Histogram of $\delta^{34}S$ values of sulphides from diamond drill core, Union Reefs prospect.

SAMPLE NUMBER	PO	ARS	SPA	PY	CCP
UR001				9.5	
UR003		6.3			
UR005		5.6			
UR008		7		7.6	
UR009		6.7			
UR020		6.2			
UR022		6.2			
UR023a				6.6	
UR023b				7.4	
UR025		6.3			
UR027a				6.7	
UR027b				7.8	
UR028				7.8	
UR029a				7	
UR029b				7.3	
UR030a			7.1		
UR030b			6.7		
UR030c			6.8		
UR035				7.7	
UR036a				7.3	
UR036b				7	
UR038				6.9	
UR041a	4.7				
UR041b	5.6			5.6	
UR043	5.3				
UR045a	6.2				
UR045b	6.8				
UR046					11.6
Average	5.7	6.3	6.9	7.3	11.6

TABLE 6.1: $\delta^{34}S$ values.

Bachinski (1969) suggested that coexisting sulphides approach isotopic equilibrium when $\delta^{34}S$ pyrite > $\delta^{34}S$ sphalerite > $\delta^{34}S$ chalcopyrite > $\delta^{34}S$ galena and also when $\delta^{34}S$ pyrite > $\delta^{34}S$ pyrrhotite, and related this to the bond strengths of the various sulphides. The average results of this study are in agreement, ie., $\delta^{34}S$ pyrite (7.3‰) > $\delta^{34}S$ sphalerite (6.9‰) and $\delta^{34}S$ pyrite (7.3‰) > $\delta^{34}S$pyrrhotite (5.7‰). This suggests that these minerals may have approached, but did not obtain, isotopic equilibrium.

Rye and Ohmoto (1974) suggested that a narrow range of $\delta^{34}S$ values is related to isotopic disequilibrium. In this case the narrow range of $\delta^{34}S$ values for pyrite, arsenopyrite, pyrrhotite and sphalerite may be related to this.

Geothermometric calculations, relative $\delta^{34}S$ and the tight range of $\delta^{34}S$ values all suggest that pyrite, arsenopyrite, pyrrhotite and sphalerite were deposited in isotopic disequilibrium. Since sulphur isotopes may not respond to the changes in the chemical environment during mineral deposition, processes such as boiling, mixing of fluids and/or redox reactions may result in isotopic disequilibrium (Rye and Ohmoto, 1974). Fluid quenching is another possible process which may result in isotopic disequilibrium (D. Huston, *pers. comm.*, 1992).

6.3 Source for sulphur

Sulphur at the Union Reefs prospect was most likely carried by mixed fluids originating from two sources. One of the sources may have been the Cullen Batholith, ie., an igneous source; $\delta^{34}S$ values for igneous rocks are 0±5‰ (Ohmoto, 1986). The other source of sulphur may have been the sedimentary pile.

Intrusion of the Cullen Batholith may have disturbed the geothermal gradient in such a manner as to produce convection cells in the surrounding country rock. Fluids circulating in these cells may have obtained sulphur from the sedimentary pile and transported it to favourable sites of deposition. The average concentration of sulphur in sedimentary rocks is 0.74% as sulphates and 0.25% as sulphides (Hoefs, 1973), indicating that this would be a likely sulphur source.

The fluids which picked up the sulphur may have been seawater, connate and/or metamorphic in origin. The average $\delta^{34}S$ value of marine sulphate during the Proterozoic was approximately 17‰ (Claypool *et al.*, 1980). Seawater sulphate from this time would have had this average value. Connate and metamorphic fluids

would have picked up sulphur from sulphate minerals (e.g., gypsum and anhydrite) precipitated from seawater percolating through the sedimentary pile.

The average value of 6.6‰ for pyrite, arsenopyrite, pyrrhotite and sphalerite is too high for an igneous source (0±5‰) alone and too low for a sedimentary source (17‰). Mixing of these two sources, the igneous being dominant, would account for this value.

The sulphur isotope results are consistent with a mineralisation event involving the intrusion of the Cullen Batholith and the development of a hydrothermal system.

6.4 Summary

(1) Average $\delta^{34}S$ = 6.6‰ for pyrite, arsenopyrite, pyrrhotite and sphalerite.

(2) Geothermometric calculations, relative $\delta^{34}S$ values and the tight range of $\delta^{34}S$ values suggests these sulphides did not obtain isotopic equilibrium during their deposition.

(3) The source for sulphur at the Union Reefs prospect is a mixture of igneous sulphur (Cullen Batholith) and sulphur derived from the sedimentary pile, the igneous sulphur being dominant.

(4) The sulphur isotope results are consistent with a mineralisation event involving the intrusion of the Cullen Batholith and the development of a hydrothermal system.

CHAPTER 7

GEOCHEMICAL MODEL FOR MINERALISATION

7.1 Geochemical conditions during mineralisation

The geochemical conditions during mineralisation, as indicated from Chapter 5 and 6 are as follows:-

1. The system is sulphur rich since at least 50% of the mineralisation is sulphidic.
2. The close relationship between marcasite and pyrite indicates a fluctuating pH centred at approximately 4.5 (Schoonen & Barnes, 1991).
3. Chalcopyrite disease is indicative of a moderate temperature (200-400°C) of sphalerite precipitation (Barton & Bethke, 1987).
4. The presence of bismuth, which has a melt point of 271°C (Hultgren *et al.*, 1973), is indicative of a maximum temperature of 271°C during precipitation of bismuth, bismuthinite, gold and the unidentified phase.
5. The indicated metal deposition sequence, as based on the paragenetic sequence, is as follows:- Fe/(Cu) => Fe/As => Fe/Cu => Pb => Au/Bi/(Cu). In accordance with models for metal zonation, as defined by Large (1991), the sequence indicates that the hydrothermal system cooled down progressively.
6. Sulphide minerals were deposited in isotopic and textural disequilibrium.

7.2 Metal/ligand source

The relative potential of greywackes and sub-greywackes to act as sources for gold (Boyle, 1979) indicates that gold at the Union Reefs prospect may have been derived from a sedimentary source, in particular, the Burrell Creek Formation. This however, does not preclude the potential of the granites as a gold source, since the presence of bismuth within the mineral assemblage is consistent with an igneous origin.

Sulphur isotope analyses indicate that sulphur was derived from a mixed igneous, and sedimentary source.

7.3 Gold transportation and deposition

The two most common gold complexes in hydrothermal fluids are $AuCl^-_2$ and $Au(HS)^-_2$. Given the sulphur rich nature of the hydrothermal system and the

temperature constraints indicated above, it is possible that gold was transported as a $Au(HS)^-_2$ complex. However, the acidity of the fluid, as indicated above, may suggest that gold was transported as a $AuCl^-_2$ complex. Hence the nature of gold transportation at the Union Reefs prospect is not clear.

Nevertheless, the association of gold with arsenopyrite (see Section 5.2), indicates that gold was deposited as a result of a decrease in the oxygen fugacity as relatively oxidised fluids interacted with relatively reduced arsenopyrite. This mechanism of gold deposition is consistent with conclusions by Huston and Large (1989) whereby gold deposition from $AuCl^-_2$ or $Au(HS)^-_2$ can be achieved through a decrease in oxygen fugacity.

7.4 Heat source

There are two possibilities for the source of heat required to produce the hydrothermal system:-

1. Heat from the emplacement of an igneous body.
2. Heat inherent from the geothermal gradient.

Several plutons occur in the vicinity of the Union Reefs prospect, namely the Bludells Monzonite, the Allamber Springs Granite, the McMinns Bluff Granite and the Tabletop Granite. The intrusion of these plutons would have caused a disruption in the local geothermal gradient at the time of their emplacement which may have resulted in convective circulation of waters within the sedimentary pile.

The relationship of the Tabletop Granite to gold mineralisation is not apparent, however, the pluton is not considered a heat source. This is because it is situated 5 km west of the prospect, and at too great a distance for convective circulation to have facilitated gold mineralisation at the Union Reefs prospect. Furthermore, the contact aureole of this pluton does not impinge on the prospect. For similar reasons the McMinns Bluff Granite is not considered a source for heat.

The relationship of the Bludells Monzonite to gold mineralisation is understood, since sulphide mineralisation is known to exist in the pluton (see Section 3.2.1). Furthermore the pluton is strongly deformed. This would indicate that the Monzonite was emplaced prior to the mineralising event and possibly prior to D1. Hence this pluton is not considered a source for heat.

There is no direct relationship between the Allamber Springs Granite and gold mineralisation at the Union Reefs prospect, however, the pluton has a close spatial relationship with the prospect. Furthermore, the prospect lies at the margin of the contact aureole of the pluton. Hence this pluton is considered a likely source of heat.

A further source for heat may be that inherent in the geothermal gradient. Sibson *et al.* (1975) suggested that fluid pressures at depth may be greatly disputed during movement along deep crustal faults. In these deep crustal faults, a high permeability channel-way is produced. This may allow fluid to rise abruptly, causing metal deposition as the fluid decompresses. Mineralisation may develop on the fault plane or in connected extension fissures at pressures of approximately 2-4 Kb (Sibson, 1989). Heat is derived from the geothermal gradient directly, rather than through disruption of the local geotherms. It is possible that a high permeability channel-way existed on the Pine Creek Shear Zone at the time of gold mineralisation at the Union Reefs prospect.

CHAPTER 8

DISCUSSION AND CONCLUSIONS

8.1 Discussion

During D_1, $\sigma 1$ was orientated east-west, and $\sigma 3$ was vertical. It is likely that a non-coaxial sinistral stress field was in operation during D_1, with sinistral movement on north-west trending faults, and dextral movement on north-easterly trending faults (X shears). The formation of buck quartz and sheeted quartz veins occurred early in D_1. These veins were folded subsequent to their formation and a foliation was developed within them at the culmination of D_1. Similarly the sediments were tightly folded and a strong near bedding parallel foliation was produced. The sediments were subjected to regional metamorphism to greenschist facies. The Bludells Monzonite was emplaced prior to this deformation and cordierite spots within the contact aureole of this pluton were deformed and elongated parallel to the S_1 fabric.

During D_2, $\sigma 1$ was orientated north-south, and $\sigma 3$ was orientated east-west. It is likely that a non-coaxial dextral stress field was in operation during D_2, with dextral movement on north-west trending faults and sinistral movement on north-easterly trending faults. The formation of breccia zones and quartz sulphide veins occurred early in D_2 when dilatant structures were formed within uplifted, fault bounded blocks and corridors. Long wavelength folds, mesoscopic folds, a discontinuous spaced and crenulation cleavage, and conjugate kinks were progressively producing in the sediments throughout D_2. A granoblastic foliation was produced in the breccia zones and quartz sulphide veins at the culmination of D_2. Pre-D_1 cordierite spots were overprinted by the S_2 foliation. The interference of F_1 and F_2 folds produced domal structures, and S_1 was folded about F_2 folds.

The formation of breccia zones and quartz sulphide veins was synchronous with mineralisation. Mineralising fluids were probably derived from a mixed igneous and sedimentary source as crustal fluids convected under the influence of elevated temperatures. It is envisaged that fluid convection and its enrichment in metal was facilitated by the emplacement of the Allamber Springs Granite. Further metal enrichment probably resulted as convecting fluid moved through the sediments of the Burrell Creek Formation. Convection was facilitated by the fractured nature of the host rock units. The convecting fluids were focussed into dilational zones (e.g. fractures within the Bludells Monzonite, buck quartz and sheeted veins and competent lithologies of the Burrell Creek Formation), and mineral precipitation

resulted from changes in fluid geochemistry. Gold precipitation possibly resulted from a decrease in oxygen fugacity associated with the interaction of gold bearing fluids with arsenopyrite. The sequence of sulphide precipitation (i.e., pyrrhotite/chalcopyrite => pyrite/marcasite => sphalerite/chalcopyrite => galena => gold/bismuth/bismuthinite/unidentified phase) indicates the convective system cooled progressively.

The deformation of sulphide minerals (and host quartz) indicates that sulphide precipitation preceded D_2. The formation of an S_2 foliation at the culmination of D_2, was concurrent with the formation of boudins in arsenopyrite, fractures in all sulphides, and granoblastic re-equilibration of quartz.

8.2 Conclusions

1. Gold mineralisation at the Union Reefs prospect is hosted within Palaeoproterozoic metasediments termed the Burrell Creek Formation.

2. It is possible to correlate lithological units through the development of a stratigraphic sequence of facies.

3. Two deformations are evident at the Union Reefs prospect :-

(i) D_1 is characterised by tight north-south folding, buck and sheeted quartz veins, stylolitic to anastomosing north-south trending cleavage in quartz veins and a slaty north-south trending cleavage in sedimentary units.

(ii) D_2 is characterised by long wavelength folds, mesoscopic folds, quartz sulphide veins, breccia zones and a discontinuous spaced cleavage

4. It is likely that a non-coaxial sinistral stress field operated during D_1, with sinistral movement on north-west trending faults (R_1 and P shears) and dextral movement on north-easterly trending faults (X shears).

5. The formation of buck quartz and sheeted quartz veins occurred early in D_1. These veins were folded subsequent to their formation.

6. It is likely that a non-coaxial dextral stress field operated during D_2, with dextral movement on north-west trending faults (P and R_1 shears) and sinistral movement on north-easterly trending faults (R_2 shears).

7. The formation of breccia zones and quartz sulphide veins occurred early in D2 when dilatant structures were formed within uplifted, fault bounded blocks and corridors.

8. The mineralisation event postdated D_1 and preceded D_2.

9. The mineralisation, in paragenetic order, consists of pyrrhotite/chalcopyrite => arsenopyrite => marcasite/pyrite => chalcopyrite => sphalerite => chalcopyrite disease => sphalerite => galena => gold/bismuth/bismuthinite/unidentified phase. Quartz, chlorite, sericite and calcite are the major gangue minerals.

10. The geochemical conditions during mineralisation were:-

(i) The system was sulphur rich.

(ii) The pH was centred at approximately 4.5.

(iii) The temperature of sulphide deposition was moderate (200-400°C).

(iv) The system cooled down progressively.

(v) Sulphide minerals were precipitated in isotopic and textural disequilibrium.

11. The source for gold may have been the sedimentary pile, but this does not preclude the granites as sources. Sulphur was derived from a mixed igneous and sedimentary source.

12. Gold may have been transported as $AuCl^-_2$ and/or $Au(HS)^-_2$. Gold deposition may have been a result of a decrease in oxygen fugacity.

13. The most likely heat source was the Allamber Springs Granite.

6. Mineralisation is controlled by the following structures:-

(i) The western limb and hinge zone of the Broken China Anticline.

(ii) The domal structure produced by the interference of F_2 and F_1 folds.

(iii) Fault bounded blocks and corridors.

(iv) The lithological packages of the Lady Alice Sandstone, Central Sandstone and Union North Sandstone.

BIBLIOGRAPHY

Bachinski, D.J., 1969. Bond strength and sulfur isotope fractionation in coexisting sulfides. ECONOMIC GEOLOGY, Volume 64, pp. 56-65.

Baxter, J.L., 1987. Structural Geology Analysis of the Union Reefs Gold Deposit, Pine Creek Geosyncline, Northern Territory. Report number: JLB 35/1987/CMS 1, Hermitage Holdings Pty. Ltd., pp. 14.

Bethke, P.M. Jr., & Barton, P.B., 1987. Chalcopyrite disease in sphalerite: Pathology and epidemiology. AMERICAN MINERALOGIST, Volume 72, pp. 451-467.

Boyle, R.W., 1979, The geochemistry of gold and its deposits. GEOPHYSICAL SURVEY OF CANADA, Bulletin 280.

Claypool, G.E., Holser, W.T., Kaplan, I.R., Sakai, H. & Zak, I., 1980. The age curves of sulfur and oxygen isotopes in marine sulphates an their mutual interpretations. CHEMICAL GEOLOGY, Volume 28, pp. 199-260.

Cox, S.F. & Etheridge, M.A., 1983, Crack-seal fibre growth mechanisms and their significance in the development of oriented layer silicate microstructures. TECTONOPYSICS, Volume 92, pp. 147-170.

Ehlers, E.G. & Blatt, H., 1982, Petrology: Igneous, sedimentary and metamorphic. W.H. Freeman and Company, pp. 732.

Etheridge, M.A., Rutland, R.W.R. & Wyborn, L.A.I., 1987, Orogenesis and tectonic process in the early to middle Proterozoic of northern Australia. AMERICAN GEOPHYSICAL UNION, Geodynamic series 17, pp. 131-147.

Ferguson, J., 1980. Metamorphism in the Pine Creek Geosyncline and its bearing on stratigraphic correlations, in: *Uranium in the Pine Creek Geosyncline* (Ed: J. Ferguson & A. B. Goleby). International Atomic Energy Agency, Vienna, pp. 91-100.

Gray, D.R., 1977. Morphological classification of crenulation cleavage. JOURNAL OF GEOLOGY, Volume 85, pp. 229-235.

Hoefs, J., 1973. Stable isotope geochemistry. Minerals, rocks and inorganic materials. Monograph series of theoretical and experimental studies, Springer-Verlag, pp. 140 p.

Hossfeld, P.S., 1936, The Union Reefs Gold-field. Aerial, Geological and Geophysical Survey of Northern Australia, Northern Territory Report No. 2., 8 p.

Hultgren, R., Desai, P.D., Hawkins, D.T., Gleiser, M., Kelley, K.K. & Wagman, D.D., 1973, Selected values of the thermodynamic properties of the elements. Published by the American Society for Metals, USA, pp. 71-80.

Ixer, R.A., 1990. Atlas of Opaque and Ore Minerals in Their Associations. Springbourne Press, Great Britain, pp. 108.

Jensen, H.I., 1915. Report on Diamond Drilling in the Northern Territory. Bulletin of the Northern Territory of Australia. Bulletin No. 12, pp. 12.

Johnston , J.D., 1984. Structural evolution of the Pine Creek Inlier and mineralisation therein, N.T., Australia. Unpublished Ph.D. thesis, Monash University.

Krowkowski, J. & Olissoff, S. 1990. The Pine Creek Shear Zone north of Pine Creek (Northern Territory) structural evolution and experimental studies. Ninth International Conference on Basement Tectonics, Geological Society of Australia, Abstract Number 26, Canberra, Australia, 2-6 July, pp. 10.

Large, R.R., 1991, Importance of mineral zonation in understanding the chemistry and processes of ore formation, in *Exploration geochemistry and hydrothermal geochemistry.* (Ed: CODES Key Centre). Master of Geology short course manual No. 12, Section 3.

Needham, R.S. & Stuart-Smith, P.G., 1985a. Revised stratigraphic nomenclature and correlation of Early Proterozoic rocks of the Darwin-Katherine region, Northern Territory. BMR JOURNAL OF AUSTRALIAN GEOLOGY AND GEOPHYSICS, Volume 9, pp. 233-238.

Needham, R.S. & Stuart-Smith, P.G., 1985b. Stratigraphy and tectonics of the Early to Middle Proterozoic transition, Katherine-El Sherana area, Northern Territory. AUSTRALIAN JOURNAL OF EARTH SCIENCES, Volume 32, pp. 219-230.

Needham, R.S., Crick, I. H. & Stuart-Smith, P.G., 1980. Regional geology of the Pine Creek Geosyncline, in: *Uranium in the Pine Creek Geosyncline* (Ed: J. Ferguson & A. B. Goleby). International Atomic Energy Agency, Vienna, pp. 1-22.

Needham, R.S., Stuart-Smith, P.G. & Page, R.W., 1988. Tectonic evolution of the Pine Creek Inlier, Northern Territory. PRECAMBRIAN RESEARCH, Volume 40/41, pp. 543-564.

Ohmoto, H., 1986. Stable isotope geochemistry of ore deposits, in: *Stable isotopes in high temperature geological processes* (Ed: J.W. Valley, H.D. Taylor and J.K. O'Neill). Mineralogical Society of America, Reviews in Mineralogy, Volume 16, pp. 491-559.

Ohmoto, H. & Rye, R.O., 1979. Isotopes of Sulfur and Carbon, in: *Geochemistry of hydrothermal ore deposits* (Ed: H.L. Barnes). John Wiley & Sons, Inc. Publishers. pp. 509-567.

Page, R.W. & Williams, I.S., 1988. Age of the Barramundi Orogeny in northern Australia by means of ion microprobe and conventional U-Pb zircon studies. PRECAMBRIAN RESEARCH, Volume 40/41, pp. 21-36.

Plumb, K.A., 1991. New Precambrian time scale. EPISODES, Volume 14, Number 2, pp. 139-140.

Powell, C. McA., 1979. A morphological classification of rock cleavage, in *Microstructural processes during deformation and metamorphism* (Ed: T.H. Bell & R.H. Vernon). TECTONOPHYSICS, Volume 58, pp. 21-34.

Ramdohr, P., 1980. The ore minerals and their intergrowths. Pergamon Press, Second Edition, pp. 1207.

Richards, J.R., Ruxton, B.P., & Rhodes, J.M., 1977. Isotopic dating of the I eucogranite, Rum Jungle, Australia. PROCEEDINGS OF THE AUSTRALASIAN INSTITUTE OF MINING AND METALLURGY, Number 264, pp. 33-43.

Robinson, B.W. & Kusakabe, M., 1975. Quantitative preparation of sulphur dioxide, for $^{34}S/^{32}S$ analyses, from sulphides by combustion with cuprous oxide. ANALYTICAL CHEMISTRY, Volume 47, Number 7, June 1975, pp. 167-168.

Rye, O. R. & Ohmoto, O., 1974. Sulfur and Carbon Isotopes and Ore Genesis: A Review. ECONOMIC GEOLOGY, Volume 69, pp. 826-842.

Schoonen, M.A.A. & Barnes, H.L., 1991, Mechanism of pyrite and marcasite formation from solution: III. Hydrothermal systems. GEOCHIMICA et COSMOCHIMICA ACTA, Volume 55, pp. 3491-3504.

Shields, J.W., 1970. Diamond Drilling at Union Reefs 1969-1970. Unpublished report to Central Pacific Minerals N.L..

Shields, J.W., White, D.A. & Ivanac, J.F., 1967. Geology of the gold prospects at Union Reefs, Northern Territory. Bureau of Mineral Resources, Geology and Geophysics. Report number 45, pp. 18.

Sibson, R.H., 1989, Structure and mechanisms of fault zones in relation to fault hosted mineralization (Unpublished). Australian Mineral Foundation, South Australia, 66 p.

Sibson, R.H., Moore, J, McM. & Rankin, A.H., 1975, Seismic pumping - a hydrothermal fluid transport mechanism. JOURNAL OF THE GEOLOGICAL SOCIETY OF LONDON, Volume 131, pp. 653-659.

Simpson, J. F., Huntington, J.F., Leishman, J. & Green, A. A., 1980. A study of the Pine Creek Geosyncline using integrated Landsat and aeromagnetic data, in: *Uranium in the Pine Creek Geosyncline* (Ed: J. Ferguson & A. B. Goleby). International Atomic Energy Agency, Vienna, pp. 141-155.

Stuart-Smith, P.G., 1985. Geology and metallogeny of the Cullen Mineral Field, Northern Territory. Unpublished Ph.D. thesis, University of New South Wales.

Stuart-Smith, P.G., 1987. Geology and Metallogeny of the Cullen Mineral Field, 1:250 000 scale map, Bureau of Mineral Resources, Canberra.

Stuart-Smith, P.G. & Page, R.W., 1991. Geochronology of Cullen Batholith, Pine Creek Inlier. BMR 91: Yearbook of the Bureau of Mineral Resources, Geology and Geophysics, Australian Government Publishing Service, Canberra, pp. 68.

Stuart-Smith, P.G., Needham, R.S., Bagas, L. & Wallace, D. A., 1987. Pine Creek, Northern Territory, 1:100 000 scale map, Bureau of Mineral Resources, Canberra.

Stubley, M.P., 1990. The geometry and kinematics of a suite of conjugate kink bands, southeastern Australia. JOURNAL OF STRUCTURAL GEOLOGY, Volume 12, Number 8, pp. 1019-1031.

Suppe, J. 1985. Principles of Structural Geology. Prentice-Hall, Inc., New Jersey, pp. 537.

Turner, I. R., 1990. Union Reefs Gold Deposits, in Geology *and Mineral Deposits of Australia and Papua New Guinea* (Ed: F. E. Hughes), The Australasian Institute of Mining and Metallurgy: Melbourne, pp. 769-771.

Walker, R.G., 1984. Turbidites and associated coarse clastic deposits, in: *Facies models* (Ed: R. G. Walker). Geoscience Canada, Reprint Series, Second Edition, pp. 171-188.

Appendix 1

Structural and lithological data

STRUCTURAL AND LITHOLOGICAL DATA LEGEND

LITHOLOGY - GRW = Predominantly sandstone greywacke.
SLT = Predominantly siltstone/shale.
AN = Interbedded anoxic units.
HSI = High degree of silicification.
MONZ = Monzonite.
GNT = Granite.
HFS = Hornfels.
GRIT = Gritstone marker.

STRIKE - Strike of feature.

DIP - Dip of feature.

DIP DIREC. - Dip direction.

SHORTENING - Shortening of folded quartz veins or bedding (original length over shortened length).

PLUNGE - Plunge of feature.

TREND - Trend of feature.

SYMBOL - S0 = Bedding.
S1 = Continous slaty cleavage.
S2 = Discontinuous spaced cleavage.
F = Fault.
FSB = Silicified fault/breccia zone.
SHR = Shear.
Va = Buck quartz veins.
Vb = Sheeted quartz veins.
Vc = Quartz sulphide veins.
Vd = Breccia zones (chloritised and silicified).
V1C and V2C = Vein cleavage.
V1F and V2F = Folded vein.
LS = Slickenslides.
LF1 = F1 Folds.
LF2 = F2 Folds.
LG = Granite lineation.
DK = Dyke.
DKV = Vein in dyke.
VM = Vein mullions.
WM = Wallrock mullions.
J = Fracture.
K = Kinks.
CK = Conjugate kinks.
CRN = Discontinuous crenulation cleavage.
APL = Air photo linear.

YOUNG - Younging direction.

COMMENT - Other information.

STRUCTURAL AND LITHOLOGICAL DATA

LITH-OLOGY	STRIKE	DIP	DIP DIREC.	SHORT-ENING	SYMBOL	YOUNG	COMMENT
	85				APL		
	289				APL		
	297				APL		
	298				APL		
	289				APL		
	296				APL		
	299				APL		
	14				APL		
	23				APL		
	39				APL		
	298				APL		
	299				APL		
	300				APL		
	300				APL		
	282				APL		
	301				APL		
	32				APL		
	358				APL		
	44				APL		
	307				APL		
	24				APL		
	352				APL		
SLTAN					K		STRIKE 203 AND 230
GRW		90	330		CRN		
GRIT		57	193		CRN		
SLT		90	215		CRN		
HSI	049	90			DK		
GNT	350	38	W		DK		GREISEN
HSI	025	90			DKV		
GRW	291				F		F NOT PROVEN
SLT	314	14	W		F		5cm displacement DEXTRAL
GRW	284	90			F		10CM DISP SINESTRAL
GRW	312	90			F		50CM DISP SINESTRAL
GRW	304	90			F		DISP? SINESTRAL
GRW	313	44	E		F		SINESTRAL
SLT	291	82	W		F		
SLT	021	90			F		SINESTRAL
GRW	015	70	E		F		SINESTRAL
GRIT	331	90			F		2m DISPLASCEMENT
GRW					F		SINESTRAL 5cm DISPLACEMENT
GRIT	051	90			F		2m DISPLACEMENT
	351	90			FSB		
	348	90			FSB		
SLT	005	90			FSB		
SLT	342	90			FSB		
	360	90			FSB		
	348	90			FSB		
	330	90			FSB		
	334	90			FSB		
	332	90			FSB		
	341	90			FSB		
	349	90			FSB		
GRW	349	90			FSB		
	338	90			FSB		
GRW	000	00			J		
GRW	278	70	SW		J		
GRW	054	51	S		J		
GRW	276	21	N		J		
GRW	295	90			J		
GRW	306	05	E		J		
GRW	324	59	E		J		
SLT	344	24	E		J		
GRW	328	27	E		J		
GRW	249	61	S		J		
GRW	089	26	N		J		
GRW	060	30	S		J		
GRW	080	22			J		
GRWAN	027	44	E		J		
SLT	068	26	S		J		

STRUCTURAL AND LITHOLOGICAL DATA

SLT	010	84	SE		J		
GRW	268	08	S		J		
SLT	025	23	S		J		
SLTAN	354	38	E		J		
SLT	327	20	W		J		
SLT	254	50	W		J		
HFS	267	79	S		J		
GRW	011	29	W		J		
GRW	012	22	W		J		
GNT	010	80	E		J		
HFS	083	85	S		J		
SLT	000	00			J		
GRW	023	40	E		J		
GRW		90	023		K		
GRW		90	167		K		
SLT		23	349		LF1		
GRW		25	332		LF1		
GRW		49	127		LF2		
SLT		90	128		LF2		
GRW		65	143		LF2		
GNT	308	90			LG		
GNT	351	90			LG		
GNT	347				LG		
GRW		13	116		LS		EBU OBLIQUE (STRIKE SLIP)
MONZ	079	41	W		LS		EAST BLOCK UP (REVERSE)
GRW	330	90			S0	WEST	
GRW	347	80	W		S0	WEST	
GRW	005	80	W		S0		
SLT	340	70	W		S0	WEST	
SLT	343	80	W		S0	WEST	
GRW	341	80	E		S0	WEST	
GRW	348	80	W		S0		
SLT	332	90			S0	WEST	
GRW	332	90			S0	WEST	
GRW	332	79	W		S0	WEST	
GRW	332	90			S0		
GRW	343	87	W		S0	WEST	
GRW	338	87	W		S0	WEST	
SLT	318	79	W		S0		
GRW	344	80	W		S0	WEST	
GRW	336	78	W		S0	WEST	
GRW	320	90			S0	EAST?	
GRW	348	82	W		S0		
GRW	321	80	W		S0	WEST	
SLT	343	88	W		S0	WEST	
GRW	294	86	E		S0	WEST?	
GRW	350	82	E		S0	WEST	
GRW	341	88	E		S0		
GRWAN	351	87	W		S0	WEST	
SLT	341	90			S0	WEST	
GRW	342	90			S0		
GRW	331	90			S0		
SLT	333	86	W		S0	WEST	
GRW	335	77	E		S0	WEST	
GRW	330	85	E		S0	WEST	
SLT	350	72	W		S0	WEST	
SLTAN	344	80	W		S0	WEST?	
GRW	337	90			S0		
GRW	343	90			S0		
SLT	350	82	W		S0		
SLT	348	90			S0	WEST	
SLT	337	90			S0		
SLTAN	335	88	W		S0	WEST	
SLT	341	83	E		S0	WEST	
GRW	341	90			S0		
GRW	086	90			S0		
SLT	325	79	E		S0		
SLT	011	70	E		S0	WEST	
SLT	338	75	E		S0		
SLT	290	90			S0		
SLT	350	84	W		S0	WEST	

STRUCTURAL AND LITHOLOGICAL DATA

GRW	332	90			S0		
GRW	317	90			S0		
HFS	360	72	E		S0		
GRW	350	78	W		S0	WEST	
GRW	334	72	W		S0		3
SLT	329	90			S0	WEST	
GRW	342	82	W		S0	WEST	
SLT	318	20	W		S0		
SLT	319	80	W		S0		
SLT	339	90			S0		
SLT	333	78	W		S0	EAST	
SLT	330	90			S0	EAST	
GRW	331	78	W		S0		
GRWAN	334	85	W		S0	WEST	
GRW	329	76	W		S0	WEST	
SLT	308	80	E		S0		
SLT	320	88	E		S0	WEST	
GRW	325	72	W		S0	EAST	
GRW	319	79	W		S0	WEST	
GRW	330	82	W		S0	WEST	
GRW	330	90			S0		
SLT	354	78	W		S0	WEST	
GRW	330	82	W		S0		
SLT	335	90			S0	EAST	
SLT	330	82	E		S0	EAST	
SLT	343	77	E		S0	EAST	
GRW	343	82	W		S0	WEST	
GRW	343	82	W		S0		
GRW	360	90			S0		
GRW	330	88	W		S0	EAST	
GRIT	335	90			S0		
GRIT	351	79	W		S0		
GRW	334	81	W		S0		
GRIT	352	90			S0		
GRW	318	64	W		S0	WEST	
SLT	325	34	E		S0	WEST	
GRIT	345	90			S0		
GRW	343	73	W		S0		
GRIT	345	90			S0		
SLT	344	68	W		S0		
GRW	331	90			S0	EAST	
HFS	333	90			S0		
HFS	332	84	W		S0		
HFS	003	90			S0		
GRW	331	88	W		S0	WEST	
GRW	327	90			S0	WEST	
GRW	329	90			S0		
GRW	348	90			S0		
HFS	002	90			S0		
GRW	324	90	W		S0		
GRW	321	90		0.64	S0		
GRW	335	82	W		S0	WEST	
GRW	344	77	W		S0	WEST	
SLT	340	88	W		S0	WEST	
GRW	339	76	W		S0	WEST	
GRW	347	68	W		S0	WEST	
SLT	331	90			S0	EAST	
GRW	342	86	W		S0		
GRW	332	90			S0	WEST	
GRW	340	87	E		S0	WEST	
SLT	334	83	E		S0	WEST	
GRW	331	85	W		S0	WEST	
GRW	035	85	E		S0		
GRW	327	88	E		S0		
GRW	301	85	E		S0		
GRW	352	74	E		S0		
GRW	334	66	E		S0		
SLT	325	90			S0	EAST	
SLT	334	90			S0	EAST	
GRW	335	90			S0	EAST	
SLT	330	90			S0		

STRUCTURAL AND LITHOLOGICAL DATA

GRW	321	90			S0		
SLT	324	90		0.80	S0		
SLT	332	90			S0	WEST	
GRW	345	90			S0		
GRIT	331	90			S0		
SLT	340	90			S0	EAST	
GRW	323	80	W		S0	EAST	
GRW	349	90			S0	EAST	
GRW	344	82	E		S0	EAST	
SLT	345	90			S0	EAST	
GRIT	340	90			S0	EAST	
SLT	327	78	W		S0	WEST	
GRIT	320	90			S0	EAST	
SLT	005	90			S0	WEST	
GRW	015	90			S0	WEST	
SLT	345	80	E		S0	EAST	
SLT	327	86	E		S0	EAST	
SLT	350	90			S0	WEST	
SLT	329	90			S0	EAST	
GRIT	329	90			S0	WEST	
GRW	360	90			S1		
SLT	008	90			S1		
SLT	358	90			S1		
GRW	348	90			S1		
GRW	355	90			S1		
GRW	328	70	W		S1		
GRW	344	90			S1		
GRW	347	90			S1		
GRW	347	90			S1		
GRW	347	90			S1		
GRW	358	90			S1		
SLT	343	90			S1		
GRW	358	90			S1		
GRW	348	90			S1		
GRW	322	90			S1		
GRW	004	90			S1		
GRW	340	90			S1		
SLT	354	90			S1		
GRW	327	90			S1		
GRW	002	90			S1		
GRW	360	90			S1		
GRW	356	90			S1		
GRWAN	001	90			S1		
GRW	360	90			S1		
GRW	359	90			S1		
SLT	009	79	W		S1		
GRW	317	90			S1		
GRW	347	90			S1		
SLT	010	80	W		S1		
SLTAN	015	90			S1		
GRW	006	90			S1		
SLT	017	90			S1		
SLT	360	90			S1		
SLT	359	90			S1		
SLTAN	360	90			S1		
SLT	014	90			S1		
SLT	026	90			S1		
SLT	010	90			S1		
SLT	009	75	W		S1		
GRW	359	90			S1		
GRW	330	90			S1		
GRW	357	68	W		S1		
SLT	010	90			S1		S2 CUTS S1
SLT	320	72	E		S1		
GRW	004	90			S1		
GRW	340	90			S1		
GRW	343	90			S1		
GRW	331	90			S1		
SLT	015	90			S1		
GRW	329	82	E		S1		
GRW	339	83	W		S1		

STRUCTURAL AND LITHOLOGICAL DATA

GRW	351	70	W		S1		
GRW	434	73	W		S1		
GRW	346	90			S1		
GRW	327	90			S1		
GRW	324	90			S1		
GRW	344	90			S1		
GRW	356	90			S1		
GRW	011	90			S1		
GRW	356	72	W		S1		
GRW	332	90			S1		
GRW	340	87	E		S1		
SLT	334	83	E		S1		
GRW	332	85	W		S1		
GRW	352	90			S1		
GRW	339	90			S1		
GRW	310	85	E		S1		
SLT	325	90			S1		
GRW	349	90			S1		
SLT	340	90			S1		
GRW	345	90			S1		
GRW	351	90			S1		
GRW	349	90			S1		
GRW	360	90			S1		
SLT	006	90			S1		
GRIT	340	90			S1		
SLT	005	90			S1		
GRW	027	90			S1		
SLT	347	82	E		S1		
SLT	329	90			S1		
GRIT	345	90			S1		
GRW	307	90			S2		
GRW	309	85	W		S2		
SLTAN	310	90			S2		
GRW	289	90			S2		
GRW	229	90			S2		
GRW	293	80	W		S2		
SLT	301	90			S2		S2 CUTS S1
SLT	001	65			S2		
SLT	339	87	W		S2		
GRW	244	71	S		S2		
GRW	015	70	W		S2		
GRW	326	90			S2		
SLT	221	90			S2		
GRW	001	82	W		S2		
GRW	015	90			S2		
GRW	289	80	W		S2		
GRW	283	90			S2		
GRW	293	90			S2		
GRW	290	90			S2		
GRW	323	90			S2		
GRW	312	52	W		S2		
SLT	292	90			S2		
GRIT	271	90			S2		
SLT	309	90			S2		
GRIT	310	90			S2		
GRW					SHR		EBU
		90	308		SHR		SINESTRAL
SLT		90	308		SHR		SINESTRAL
GRW		90	208		SHR		SINESTRAL
GRW					SHR		EBU
GRW	010	90			VA		
GRWAN	351	87	W		VA		
SLT	334	78	E		VA		
GRW	330	90			VA		
SLT	311	70	W		VA		
SLT	343	85	W		VA		
SLT	335	90			VA		
GRW	343	90			VA		
GRW	343	90			VA		
SLT	344	88	W		VA		
GRW	350	90			VA		

STRUCTURAL AND LITHOLOGICAL DATA

SLT	350	78	E		VA		
GRW	348	50	W		VA		
GRW	335	90			VA		
SLT	350	90			VA		
GRW	341	44	E		VA		
GRW	356	90			VA		
GRW	331	90			VA		
HFS	333	90			VA		
GRW	344	77	W		VA		
SLT	333	90			VA		
GRW	335	90			VA		
GRW	321	90			VA		
GRW	010	31	W		VAC		
GRW	314	28	W		VAC		
GRW		40	341		VAF		
GRW	310	78	E		VB		
SLT	332	90			VB		
SLT	342	75	W		VB		
GRW	327	46	E		VB		
GRW	332	90			VB		
GRW	039	70	W		VB		
GRW	342	80	E		VB		
GRW	290	69	E		VB		
GRW	332	80	E		VB		
SLT	320	79	W		VB		
GRW	340	85	E		VB		
GRW	316	86	E		VB		
GRW	282	60	W		VB		
GRW	331	70	W		VB		
GRW	330	78	E		VB		
GRW	005	90			VB		
GRW	008	90			VB		
GRW	331	90			VB		
GRW	350	42	E		VB		
GRW	295	65	E		VB		
GRWAN	002	90			VB		
GRW	289	69	E		VB		
SLT	009	90			VB		
SLTAN	342	62	W		VB		
SLT	343	90			VB		
SLT	350	80	W		VB		
SLT	345	82	W		VB		
SLT	049	68	W		VB		
GRW	345	72	W		VB		
HFS	327	23	W		VB		
GRW	352	41	W		VB		
GRW	344	45	W		VB		
SLT	345	90			VB		
GRW	297	70	E		VB		
GRW	012	22	W		VB		
GRW	013	73	W		VB		
GRW	341	29	E		VB		
GRW	352	77	W		VB		
GRW	332	76	E		VB		
GRW	321	80	E		VB		
GRW	017	78	E		VB		
GRW	346	45	E		VB		
GRW	330	90			VB		
SLT	331	86	W		VB		
GRW	011	90			VB		
GRW	330	79	E		VB		
GRW	300	76	W		VB		
GRW	280	90			VB		
GRW	009	90			VB		
GRW	293	81	W		VB		
GRW	030	90			VBC		
SLT	025	00			VBC		
GRW	071	90			VBC		
GRW	351	54	W		VBC		
SLT	255	22	N		VBC		
SLT	333	36	E		VBC		

STRUCTURAL AND LITHOLOGICAL DATA

GRW	252	59	S		VBC		
GRW	074	35	E		VBC		
GRW	357	20	W		VBC		
GRW	064	10	N		VBC		
GRW		40	331	0.50	VBF		
GRW		40	345	0.76	VBF		
GRW		40	342	0.56	VBF		
GRW		45	340	0.56	VBF		
GRW		48	342	0.44	VBF		
GRW		45	341		VBF		
GRW		31	332		VBF		
GRW		42	338		VBF		
GRW		50	340		VBF		
GRW				0.48	VBF		
GRW		49	340		VBF		
GRW	286	90			VC		
GRW	062	90			VC		
SLT	318	79	W		VC		
SLT	280	79	W		VC		
GRW	345	80	E		VC		
SLT	324	60	W		VC		
GRW	350	82	E		VC		
GRWAN	018	80	E		VC		
GRWAN	027	44	E		VC		
GRW	331	90			VC		
SLTAN	325	77	E		VC		
MONZ	009	83	E		VC		
SLT	074	50	W		VC		
GRW	329	35	W		VC		
GRW	329	18	E		VC		
GRW	321	80	E		VC		
GRW	010	90			VD		
GRW	341	90			VD		
GRW	331	90			VD		
GRW	354	90			VD		
GRW	345	90			VD		
SLT	350	90			VD		
SLT	350	90			VD		
SLT	349	90			VD		
SLT	331	90			VD		
GRW	332	90			VD		
GRW	331	70	W		VD		
GRW	343	90			VD		
SLT	330	90			VD		
GRWAN	335	90			VD		
SLT	325	34	E		VD		
GRW	343	70	W		VD		
SLT	335	70	W		VD		
GRW	331	90			VD		
GRW	331	85	W		VD		
GRW	330	90			VD		
GRW	015	90			VD		
GRW		10	329		VM		
SLT	334	00			VM		
SLT		18	311		VM		
SLT		19	343		VM		
GRW		17	321		VM		
SLT		15	350		VM		
SLT							
GRW							
HSI							

CALCULATED S0/S1 INTERSECTIONS

PLUNGE	TREND
66	1
52	4
79	18
36	27
0	84
67	112
76	128
52	137
7	151
59	158
60	160
64	162
57	163
52	166
52	167
44	167
82	168
90	169
81	173
80	174
84	174
67	174
34	175
54	177
52	177
73	180
58	183
61	183
68	183
52	188
63	190
70	193
71	196
57	205
62	208
80	306
76	315
55	321
62	327
45	333
46	334
84	336
65	336
81	343
36	349
75	350

Appendix 2

Sulphur isotope data

SULPHUR ISOTOPE DATA AND CALCULATION TABLE 1

MINERAL	SAMPLE NUMBER	BOTTLE NUMBER	DELTA	delta 34Scdt
ASP	UR003	1	2.661	6.267304
ASP	UR005a	2	2.069	5.637416
ASP	UR008	3	3.375	7.027
ASP	UR009a	4	3.037	6.667368
ASP	UR020	5	2.614	6.217296
ASP	UR022a	6	2.63	6.23432
ASP	UR025	7	2.654	6.259856
CP	UR046a	9	8.447	12.423608
CP	UR046b	8	6.194	10.026416
CP	UR046c	10	9.925	13.9962
PY	UR008	16	3.948	7.636672
PY	UR023a	15	2.996	6.623744
PY	UR027a	14	3.061	6.692904
PY	UR029a	13	3.299	6.946136
PY	UR036a	12	3.611	7.278104
PY	UR038	11	3.236	6.879104
SPHAL	UR030a	19	3.446	7.102544
PYRR	UR041a	20	1.1703	4.6811992
PYRR	UR043	21	1.718	5.263952
PYRR	UR045a	22	2.627	6.231128

MEASURED VALUE	STANDARD VALUE
-2.611	0.7
8.471	12.4
11.004	15.2
0.005	3.4

SULPHUR ISOTOPE DATA AND CALCULATION TABLE 2

MINERAL	SAMPLE NUMBER	BOTTLE NUMBER	DELTA	delta 34Scdt
CP	UR046d	23	5.286	9.257736
CP	UR046e	24	10.034	14.366584
CP	UR046f	25	5.265	9.23514
PY	UR001	28	5.528	9.518128
PY	UR023b	29	3.535	7.37366
PY	UR027b	30	3.941	7.810516
PY	UR028	31	3.883	7.748108
PY	UR029b	32	3.459	7.291884
PY	UR035	33	3.874	7.738424
PY	UR036b	34	3.182	6.993832
PY	UR041	35	1.893	5.606868
SPHAL	UR030b	26	2.88	6.66888
SPHAL	UR030c	27	2.986	6.782936
PYRR	UR041b	37	1.853	5.563828
PYRR	UR045b	36	3.035	6.83566

MEASURED VALUE	STANDARD VALUE
10.727	15.2
-2.759	0.7
-0.061	3.4
8.284	12.4

Appendix 3

Sample catalogue

SAMPLE CATALOGUE LEGEND

HOLE I.D, - Diamond drill hole number

STATUS -
TS = Thin section.
TSL = Thin section large.
PB = Polished block.
PTS = Polished thin section.
SI = Sample used for sulphur isotope analyses.

DATE - Date collected.

CORE SAMPLES

SAMPLE NUMBER	DATE	HOLE I.D.	DEPTH (m)	STATUS	Description/other
UR001	13-14/2	UJ9	24.85		PY, ASP, BUK QTZ
UR002	13-14/2	UJ9	33.20	TS	GRITSTONE MARKER
UR003	13-14/2	UJ9	54.30	PTS,SI	ASP, BUK QTZ, SLT
UR004	13-14/2	UJ9	53.40	TS	ASP, QTZ, YELLOW STAINING
UR005	13-14/2	UJ9	68.30	PTS,SI	ASP,PY,CHL,QTZ
UR006	13-14/2	UJ9	75.30	TS,SI	ASP VEINS
UR007	13-14/2	UJ9	77.10	TS	ASP,PY,CHL,QTZ
UR008	13-14/2	UJ9	104.45	PTS,SI	ASP,PY,BUK QTZ
UR009	13-14/2	UJ9	104.45	PTS,SI	ASP,PY,(BRECCIA),6.1 G/T
UR010	13-14/2	UJ11	13.80		FOLD QTZ (CROC.TEXTURE)
UR011	13-14/2	UJ11	78.30		FOLD QTZ
UR012	13-14/2	UJ21	56.45		OXIDISED Fe ON BUK QTZ
UR013	13-14/2	UJ21	78.60		VIS GOLD IN BUK QTZ
UR014	13-14/2	UJ11	98.10	TS	CARB,QTZ,CHL
UR015	13-14/2	UK32	48.80	TS	STCKWRK QTZ
UR016	13-14/2	UK32	45.60		OXIDISED FE ON BUK QTZ
UR017	13-14/2	UK37	88.80	TS/PTS	QTZ,SULP VEINS,CARB VERT/272
UR018	13-14/2	UK37	88.30	TS	STEPPED' QTZ VEIN VERT/260
UR019	13-14/2	UK15	60.50		BRECCIA ZONE,SULPH
UR020	13-14/2	UK15	64.20	PTS,SI	SULP,QTZ,CHL
UR021	13-14/2	UK25	26.50	TS	OXIDISED HIGH GRADE >3G/T
UR022	24/6	URD007	110.95	PTS,SI	ASP,GAL,WALLROCK,BRECCIA BUK QTZ
UR023	24/6	URD007	168.20	PTS,SI	PY VEIN IN GRW
UR024	24/6	URD007	208.20	TSL	ASP,PINCH AND SWELL VEIN
UR025	24/6	URD007	218.50	SI	GAL,CHL,BRECCIA ZONE
UR026	24/6	URD007	220.50	SI	SPHAL,ASP,BUCK QTZ
UR027	24/6	URD007	235.80	SI	PY,ASP
UR028	24/6	URD007	237.50	PTS	QTZ VEIN,WALLROCK
UR029	24/6	URD007	245.00	PTS,SI	PY,ASP,BRECCIA ZONE
UR030	24/6	URD007	217.00	PTS,SI	SPHAL,GAL
UR031	24/6	URD007	129.40	TS	PORPHYROBLASTS
UR032	24/6	URD006	79.40		VUGGY VEIN,DISSEM ASP
UR033	24/6	URD006	138.50	TS	FOLDED/FAULTED QTZ VEIN
UR034	24/6	URD006	149.50	TS	STCKWRK VEINS
UR035	24/6	URD006	148.40	PTS	QTZ (INFILL?)
UR036	24/6	URD008	82.95	SI	PY,VUGS,QTZ
UR037	24/6	URD008	120.50	TS	BRECCIA QTZ(TRANSLUCENT)
UR038	24/6	URD008	122.50	PTS,SI	PY,CARB,QTZ,CARB
UR039	24/6	URD008	124.00	PTS	DISSEM ASP ,ASP
UR040	24/6	URD008	150.40	PTS	SPHAL,PY,BRECCIA ZONE
UR041	24/6	URD009	142.40	PTS,SI	PYRR,IN FOLDED VEIN, MAG SUS 1500
UR042	24/6	URD009	142.60	TS	PINCH AND SWELL QTZ BED PARALLEL
UR043	24/6	URD009	150.00	PTS,SI	PYRR,PY, BRECCIA ZONE
UR044	24/6	URD009	158.20	PTS	CP,PY,PYRR IN PINCH AND SWELL QTZ
UR045	24/6	URD009	179.50	PTSX2,SI	PY ,CARB,QTZ
UR046	24/6	URD007	259.00	PTS,SI	CP BRECCIA ZONE

FIELD SAMPLES

SAMPLE NUMBER	DATE	STATUS	Description/other
GRUR001	20-May	TS	TABLETOP GRANITE
GRUR002	20-May		McMINNS BLUFF GRANITE
BCUR003	20-May	TS	HORNFELS
GRUR004	20-May	TS	ALLAMBER SPRINGS GRANITE
BCUR005	20-May		HORNFELS
GRUR006	20-May		ALLAMBER SPRINGS GRANITE
MBUR007	20-May		MOUNT BONNIE FM. CHERT
GRUR008	20-May	TS	McMINNS BLUFF GRANITE DYKE
GRUR010	21-May		TABLETOP GRANITE
BCUR011	21-May		GRW (VOLCANOLITHIC?)
BCUR012	22-May		GRAPHITIC SLT
BCUR013	22-May	TSL,PB	FSB
BCUR014	22-May	TS,PB	FSB
BCUR015	22-May		FSB
BCUR016	25-May		GREEN MINERAL (EPIDOTE?) IN QTZ
DLUR017	26-May		DOLERITE POD (ORIENTED FIBER VEINS)
MBUR018	26-May		HORNFELS (FINE GRAINED)
DLUR019	2-Jun	TS	VEINS IN DOLERITE 83/009E
BCUR020	3-Jun		FSB
DLUR021	3-Jun	TS	DOLERITE
BCUR022	4-Jun		GRITSTONE MARKER (ORIENTED)
BCUR023	4-Jun	TS	GRITSTONE MARKER
BCUR023	9-Jun	TS	GRW 78/332W
BCUR025	9-Jun		SLT 78/332W
BCUR026	9-Jun	TS	SPOTTED HORNFELS
GRUR027	9-Jun		GRIESSEN DYKE 38/350W
BCUR028	10-Jun		BRECCIATED HORNFELS
BCURO29	10-Jun		BRECCIA SILICIC GRANITE
GRUR030	10-Jun		GRANITE POD (ALLAMBER SPRINGS)
DLUR031	10-Jun		DOLERITE
DLUR032	10-Jun		FN GR DOL WITH QTZ VEIN
BCUR033	11-Jun		GRW 80/347W
BCUR034	11-Jun		ANOXIC GRW 80/347W
BCUR035	11-Jun		SLT, QTZ VEIN
VCUR 036	11-Jun		BITS OF QTZ SULP VEIN 75/342W
BCUR037	14-Jun	TSL	CRENULATED SLT, W FACE 65/340W
			S FAC 88/243S
BCUR038	15-Jun		SLICKS E FACE 74/346W
			SE FACE 88/243S
ALUR039	15-Jun		ALLUVIUM
GRUR040	16-Jun	TS,PB	McMINNS BLUFF GRANITE
GRUR041	26-Jun		GRW WITH CORDIERITE SPOTS, QTZ VEIN
URA	26-Jun	TS	CRACK SEAL/BUK QTZ CROSSCUT